ACS OMEGA

Open Access

http://pubs.acs.org/journal/acsodf

Article

Modulation of MAPK/NF-κB Pathway and NLRP3 Inflammasome by Secondary Metabolites from Red Algae: A Mechanistic Study

Published as part of the ACS Omega virtual special issue "Phytochemistry".

Asmaa Nabil-Adam, Mohamed L. Ashour,* and Mohamed Attia Shreadah

Cite This: *ACS Omega* 2023, 8, 37971−37990

Read Online

ACCESS | Metrics & More | Article Recommendations | Supporting Information

ABSTRACT: The pharmacological properties of seaweeds are diverse. No studies have been conducted on the protective effect of *Galaxaura oblongata* (GOE) against lippopolysaccharide (LPS)-induced inflammation in the brain. This study is divided into three phases, the first of which is the initial phase. In vitro study includes antioxidant, radical scavenging, and anti-inflammatory activities, including cyclooxygenase-1 (COX1), COX2, NO, acetylcholine inhibition, sphingosine kinase 1, tumor necrosis factor α (TNF-α), and interleukin-6, as well as antioxidant and radical-scavenging activities, including 2,2-diphenyl-1-picrylhydrazyl and 2,2′-azinobis(3-ethylbenzothiazoline)-6-sulfonic acid. Using LPS-induced acute inflammation, the second phase was conducted in vivo. Antioxidant and anti-inflammatory assays were performed to investigate the protective role of GOE. In addition to the phytochemical analysis, the bioactive content of GOE was also investigated. In vitro results demonstrated the potential of GOE as an antioxidant, anti-inflammatory, and neuroprotective agent. A study using LPS as an induced lung injury and neuroinflammation model confirmed the in vitro results. The GOE significantly reduced inflammatory, oxidative, and neurodegenerative biomarkers based on histopathological and immuno-histochemistry results. Based on computational drug design, four target proteins were approved: nuclear factor κB, mitogen-activated protein kinases, TNF-α, and NLRP3. Using polyphenolic compounds in GOE as ligands demonstrated good alignment and affinity against the three proteins. Finally, the current study offers a new approach to developing drug leads considering GOE's protective and curative roles.

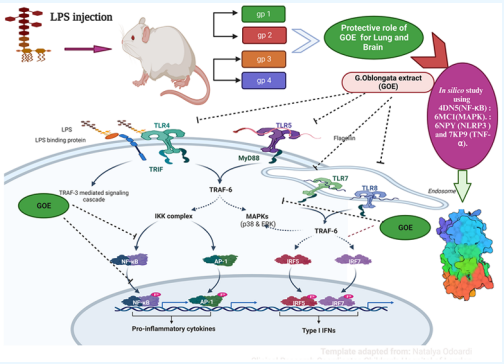

INTRODUCTION

Infections caused by bacteria are most often associated with respiratory disorders, such as acute lung injury (ALI), acute respiratory distress syndrome (ARDS), and acute exacerbations of chronic obstructive pulmonary disease (COPD). Additionally, COVID-19-infected β-coronaviruses cause extreme acute respiratory syndrome.[1] Lipopolysaccharides (LPS) are the most dangerous cell wall part among Gram-negative bacteria. Cell wall membranes of Gram-negative bacteria contain the biologically active endotoxin LPS found on their surface.[2] LPS are integral to almost all Gram-negative bacteria's outer surface membrane composition anchored by polysaccharide cores and carbohydrate chains. Lipid A is responsible for the potent immunostimulatory property of LPS.[3]

LPS may stimulate toll-like receptor 4 (TLR4) transmembrane proteins.[4] TLRs are responsible for key inflammatory responses. To display signaling *pathways* that activate other molecules, including IRAK1, IRAK4, TBK1, and Ikki protein kinases, the LPS pathogenicity mechanism binds to TLR4, which then forms transient ternary complexes with three distinct extracellular proteins, namely, LBP, CD14, and MD-2. Enhancing the production of free radicals, cytokines, and other pro-inflammatory mediators in brain, blood, and other tissues will enhance the signal in the tissue and the downregulation or upregulation of genes that orchestrate the inflammatory response.[5] LPS acts as a pro-inflammatory molecule that stimulates innate immune cells. In different cell types, TLR4 stimulates the release of interleukin 8 and other inflammatory cytokines, leading to an acute inflammatory response to pathogens. The expression of TLRs, as well as localization, is regulated in response to specific pathogens or damaged molecules. To develop a strategy for therapeutic modulation, it is crucial to understand the pro-inflammatory cytokine signaling pathways involved in controlling a pathogen.[6]

LPS is one of the most important ways to induce inflammation. A Gram-negative bacteria's outer membrane

Received: May 18, 2023
Accepted: August 21, 2023
Published: October 5, 2023

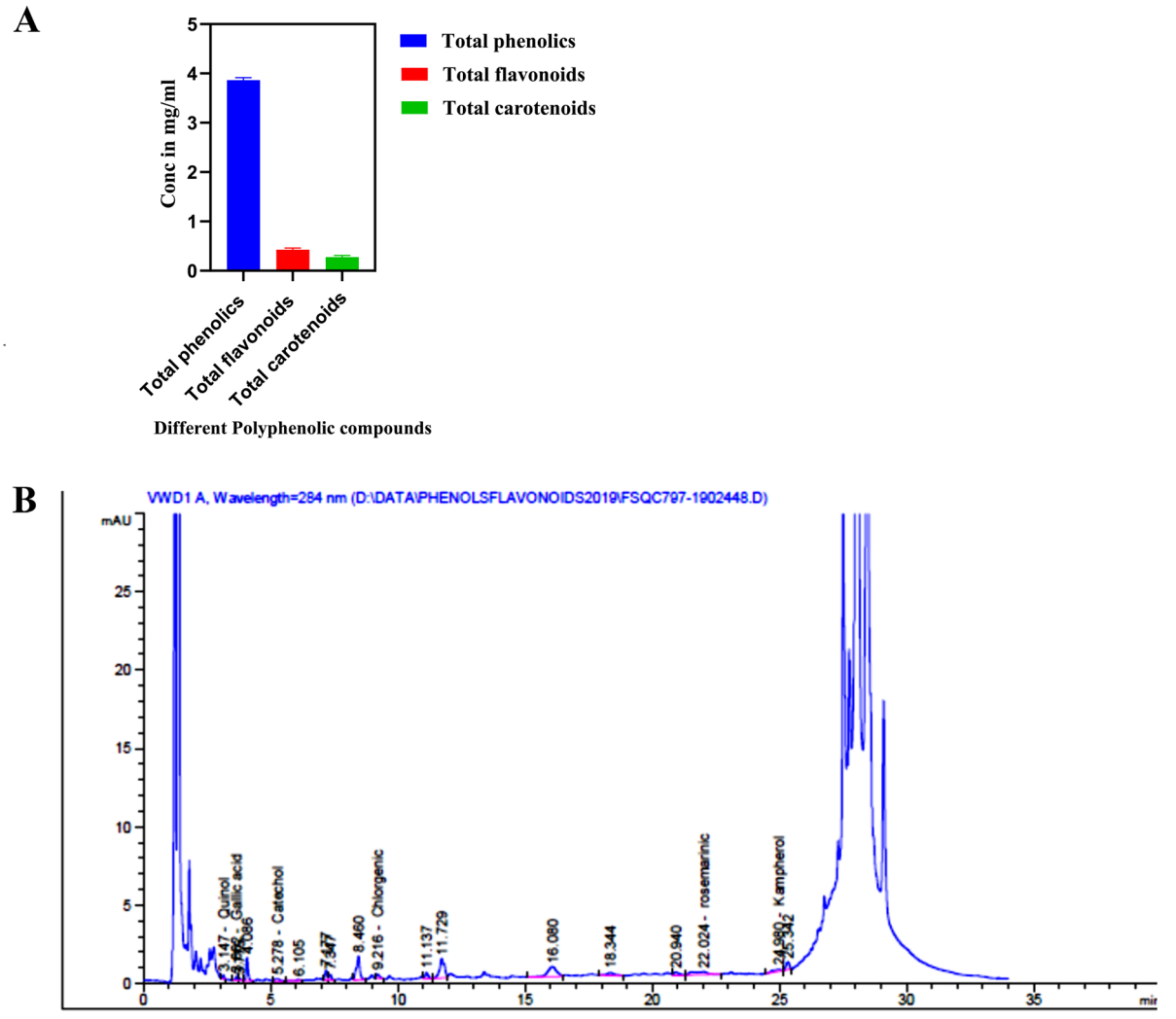

Figure 1. (A) Phytochemical analysis of the GOE. (B) HPLC chromatogram of GOE.

contains LPS. It primarily targets TLR4 but also acts on other receptors. LPS recruits downstream adapters that are crucial to signaling TLR4 upon activation. This recruitment of adaptors can trigger downstream pathways and transcription factors, activating pro-inflammatory genes.[4] It is predominantly expressed in glial cells, mainly microglia, but neurons also express TLR4. Upon activation of this receptor, neurons release different inflammatory mediators. Many in vitro and in vivo experiments use LPS.[3]

TLR4 responses are triggered when adaptor proteins activate TLR signaling. A major step in regulating gene expression is mediated through the transduction pathways activated by NF-κB and AP-1 signals.[7] Inflammatory models have extensively used bacterial LPS because they replicate many cytokines that cause inflammation, including TNF-α, IL-1, and IL-6. As a result of LPS signaling, TLR4 is responsible for transmitting it. By binding to TLR4, LPS activate MyD88 and IL-1R kinases, activating NF-κB. (IRAK). The transcription of genes in innate immunity and inflammation is controlled by multiple pathways, including TNF-associated factor 6 (TRAF-6) and NADPH oxidase (NOX) NF-kB. Several studies have shown that reactive oxygen species modulate lung and monocyte immunity.[8] Phosphoinositide 3-kinase is essential for reducing inflammation in several studies looking for new anti-inflammatory drugs. There are numerous habitats and endemic species in Egyptian marine ecosystems (17% in the Red Sea), revealing high marine biodiversity (approximately 5000 species) due to the vast areas covering more than 3000 km of distinguished coastlines with rich and diverse habitats. In Red Sea habitats, many marine organisms are exposed to extreme conditions,[9] producing unique and novel bioactive compounds with potent pharmacological properties. The Red Sea marine environment is a unique and rich natural resource for many bioactive substances with unique structural features due to its phenomenal biodiversity. Marine bioactive compounds, including marine plants, macro- and microalgae, microorganisms, and sponges, can be derived from various sources containing their own unique set of biomolecules.[10−17] Macroalgae, or seaweed, are found in tropical waters and intertidal regions. They are rich in interesting bioactive components, including vitamins, hormones, carotenoids, etc., showing potential positive uses in healthcare.[18−22] The study aims to investigate the protective effect of *Galaxaura oblongata* (*G. oblongata*; GOE), as a new marine species not investigated before, on the lung and brain using several in vitro and in vivo studies supported by histopathology and immuno-histochemistry study, and all that was confirmed using broad in silco study on several proteins.

https://doi.org/10.1021/acsomega.3c03480
ACS Omega 2023, 8, 37971−37990

RESULTS

Phytochemical Analysis. The phytochemical analysis of GOE is shown in Figure 1A). The polyphenolic constituents were 3.83 and 0.4 mg/mL for phenolics and flavonoids, respectively. Furthermore, the total carotenoids were found to be 0.25 mg/mL.

HPLC Analysis. The HPLC analysis of GOE (ethyl acetate) revealed the presence of gallic acid (3.01 mg/kg), chlorogenic acid (1.45 mg/kg), quinol (2.42 mg/kg), rosmarinic acid (112.1 μg/g), and amphorae (22.5 mg/kg), as shown in Figure 1B, Figure 2, and Table 1.

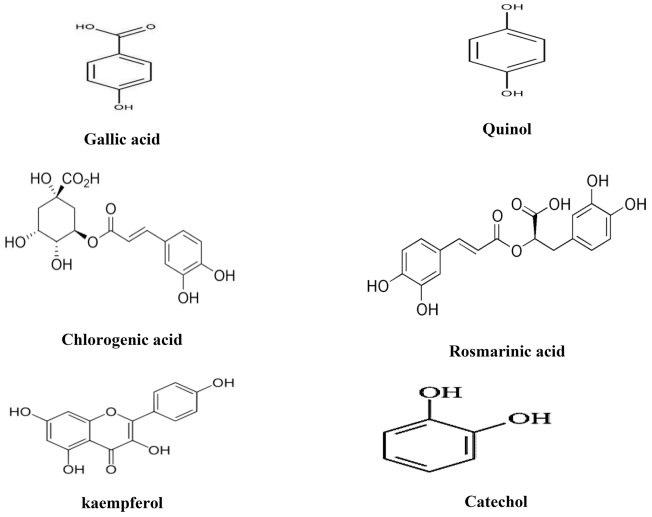

Figure 2. Structures of various compounds in the GOE extract.

Table 1. HPLC Chromatogram of GOE for Polyphenolic Compounds (Phenolics and Flavonoids)

Compound	Retention Time (min)	Amount (mg/kg)
Quinol	3.147	2.41807
Gallic acid	3.662	3.01185
Chlorogenic acid	9.216	1.45409
Rosmarinic acid	21.024	112.16214
Kaempferol	24.980	22.50129

GC-MS Analysis. The GOE's lipidomics profile resulted in various fatty acids (saturated and unsaturated). The unsaturated fatty acids were *cis*-13,16-docasadienoic acid, methyl 20-methylheneicosanoate, *cis*-11,14-eicosadienoic acid, methyl eicosanoate, linoleic acid, methy l,9-octadecenoate, and *cis*-10-heptadecenoic acid, with 22.39725309, 25.61323055, 5.774410003, 7.453204915, 1.98853199, 23.87146368, and 197.8621685 ppb, respectively, while the saturated fatty acids were methyl 20-docosanoate, methyl tetracosanoate, methyl heneicosanoate, *cis*-9,10-epoxystearic acid, stearic acid, methyl 14-methyl hexadecanoate, hexadecanoic acid (palmitic acids), octadecenoic acid (oleic acid), pentadecanoic acid, methyl myristate, myristic acid, lauric acid, tridecanoic acid, undecanoic acid, decanoic acid (capric acid), methyl-trans-tetradecanoate and octanoic acid (caprylic acid) with 11.55903959, 10.93611393, 5.590166622, 0.993889671, 176.0288411, 197.8621685, 0.658142466, 8.270176484, 7.65510775, 24.97676353, 10.85595195, 14.349048557, 755440442, 22.48978612, 2.244112595, 71.07185414, 59.77704892, 22.39725309, 25.61323055, 5.774410003, 7.453204915, 1.98853199, 23.87146368 and 197.87 ppb, respectively. Additionally, the saturated fatty acid content was 94 5% in the GOE at 633.1 ppb and the unsaturated fatty acid content was 6% at 40.71 ppb (Figure 3).

Antioxidant Capacity. The total antioxidant capacity of GOE using DPPH is shown in Figure 4A). GOE gave higher activity, with 83.01% DPPH at 10 mg.

Interleukin and Inflammatory Biomarkers. The activity of the anti-inflammatory profile of the GOE was investigated using TNF-α, COX1, and COX2 at 81%, 88%, and 83.75%, respectively, at 25 mg. Additionally, the anti-inflammatory biomarker NO was investigated using different concentrations from 10 to 1 mg, as shown in Figure 4B. The GOE gave a higher inhibition ratio of 74.5% at 10 mg of GOE.

Antiviral Activity. The antiviral activity of GOE using the reverse transcriptase enzyme was 94.5% at 25 mg of GOE (Figure 4C).

Anticancer Activity. The anticancer activity of GOE was examined using PTK inhibition. The anticancer activity was 85.70% at 25 mg of GOE (Figure 4C).

Anti-Alzheimer's Activity. The bioactivity of GOE against acetylcholinesterase was investigated at different concentrations from 1 to 10 mg. The extract of GOE exhibited higher inhibition at 10 mg (98.25%) of GOE (Figure 4D).

Impacts of GOE on the Lipid Profile Status. GOE altered the lipid profile (triglycerides and cholesterol) in the toxicity group (induction second group) and all experimental groups (Figure 5). The triglyceride was reported to be increased markedly in the second group by 91.3% compared to that of the first group (93.67 ± 4.80 vs 178.32 ± 23.88; *, $p < 0.001$). Administration of GOE in the fourth group dropped markedly in triglycerides by 40.9% with respect to that of group II (induction group) (178.32 ± 23.88 vs 114.85 ± 6.80; *, $p < 0.001$). In addition, the administration of GOE in the fourth group resulted in a nonsignificant reduction in the triglyceride level from 93.67 ± 4.80 to 91.39 ± 6.45. The total cholesterol levels were markedly increased in the second group by 77.9% compared to that of the control (53.56 ± 12.05 vs 242.57 ± 35.64). Administration of GOE in the third group revealed a marked diminished total cholesterol level by72.5% compared to that in group II (from 242.57 ± 35.64 to 66.60 ± 16.36). Furthermore, the administration of GOE alone in group IV revealed a nonmarked decrease compared to that of group I (−ve control) (53.56 ± 12.05 vs 54.27 ± 2.83), the same results for LDL and VLDL. In contrast, the results of HDL in the induction group decreased significantly compared with those of the control.

Impacts of GOE on the LPS Oxidant/Antioxidant Status. Figure 6 displays the impact of GOE on the lung LPO level and the induced toxicity group's total antioxidant biomarker activities (TAOs). The levels of LPO were significantly elevated in mice from group II by 23.28% compared to animals from group I (0.56 ± 0.05 vs 0.73 ± 0.04; *, $p < 0.001$). In comparison with that of the second group, the administration of GOE in group III demonstrated a significant reduction in LPO of 24.6% (0.55 ± 0.03 nmol/(g of liver) vs 0.73 ± 0.04 nmol/(g of liver); *, $p < 0.001$). In addition, the administration of GOE alone in group IV resulted in a little but insignificant rise in the LPO level in the lung, which went from 0.56 ± 0.05 (vs 0.73) to 0.57 ± 0.04. Compared to those found in group I, the levels of lung antioxidant biomarkers reduced after LPS treatment (group II), going from 0.46 ± 0.05 to 0.21 ± 0.06, respectively.

https://doi.org/10.1021/acsomega.3c03480
ACS Omega 2023, 8, 37971−37990

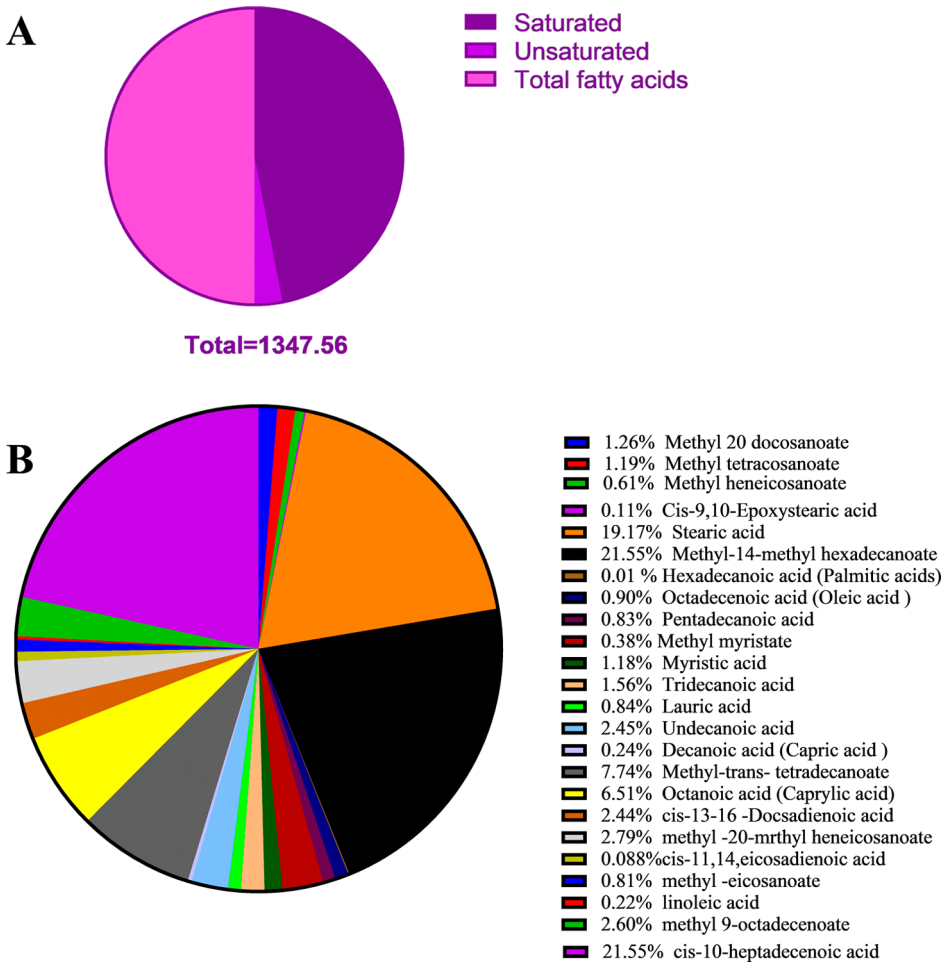

Figure 3. GC-MS analysis of GOE. (A) Total content of fatty acids. (B) Different constituents of fatty acids.

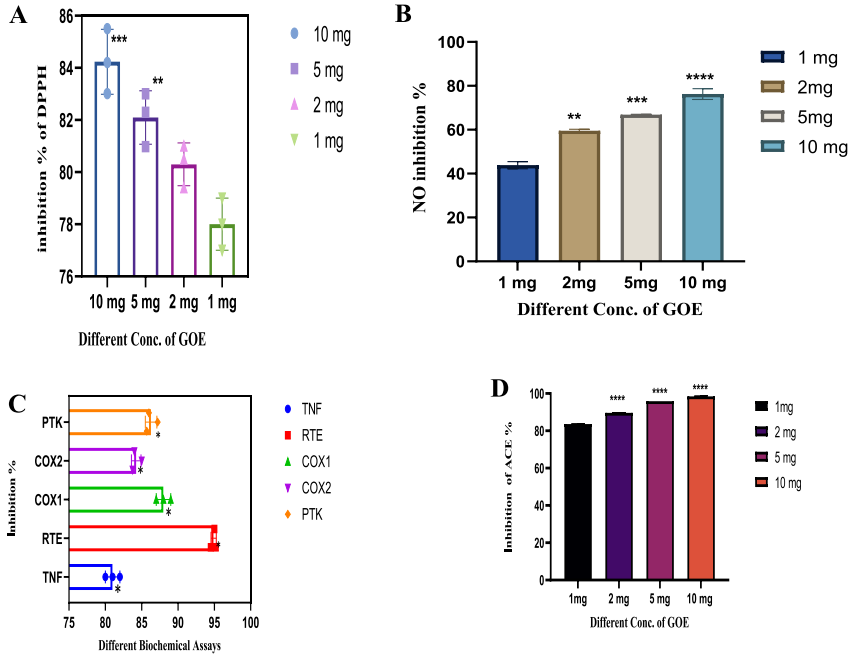

Figure 4. (A) Total antioxidant capacity of GOE using DPPH. (B) Anti-inflammatory activity of GOE using NO. (C) Anticancer (PTK), anti-inflammatory (COX1, COX2, and TNF), and antiviral (RTE) activity of inhibition. (D) Anti-Alzheimer activity of GOE using acetylcholinesterase enzyme (ACEI).

https://doi.org/10.1021/acsomega.3c03480
ACS Omega 2023, 8, 37971−37990

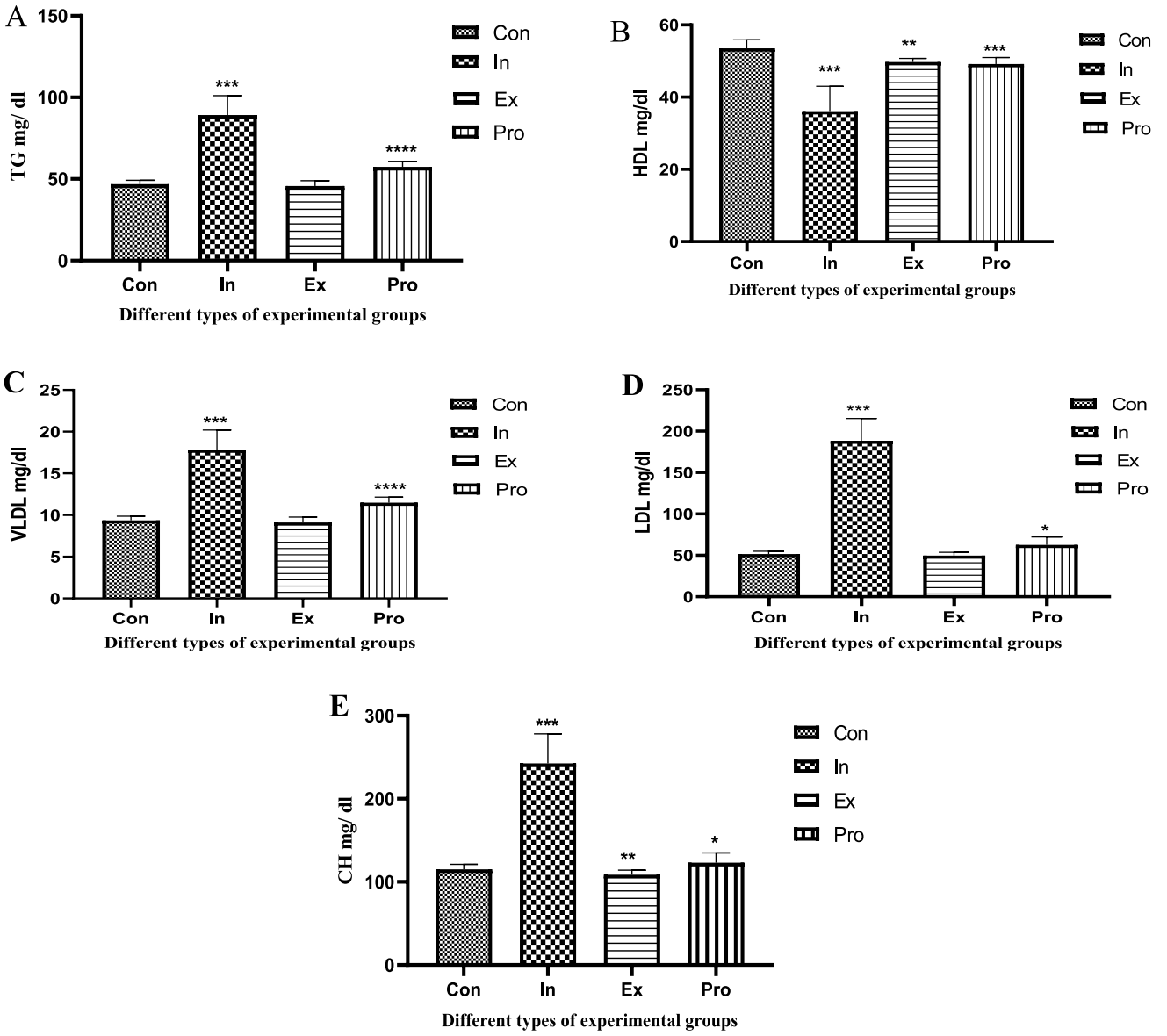

Figure 5. Effect of GOE on the lipid profiling levels, i.e., (A) TG, (B) HDL, (C) VLDL, (D) LDL, and (E) CH.

Compared to those in group II, the total antioxidant capacity of group III mice dramatically increased by 64.4% when GOE was given to the mice before they were injected with LPS.

Impacts of GOE on Inflammatory Biomarkers. *SAA Biomarkers.* The role of GOE on the activities of SAA (lung) in the LPS-treated mice group (second) relative to other experimental groups (first, third, and fourth) is represented in Figure (7). In the LPS-treated mice group (second), the activity of SAA (19897.39 ± 3493.32) increased significantly in comparison with the control group (first group) (9620.68 ± 447.00). In contrast, the pretreatment GOE (group IV) had a considerably lower SAA by 24.6.5% (25344.5 ± 2733.5) compared to that of group II.

NF-κB Biomarkers. The effect of GOE on the activities of NF-κB in (lung) in the LPS-treated mice group (second) in comparison to other experimental groups (first, third, and fourth) is shown in Figure 7. The activity of NF-κB in group II (12.93 ± 2.73) was significantly increased by 76.1% (6.43 ± 0.41) compared with that of the first group. In contrast, compared to group II, pretreatment with GOE (group IV) significantly reduced NF-κB by 35% (8.25 ± 1.03). Additionally, the NF-κB expression showed a nonmarked change in the other group.

MPO Biomarkers. The GOE effect on MPO activity (lung) in mice treated with the LPS group (second) compared to other experimental groups (I, III, and IV) is shown in Figure 7. In the treated mice with the LPS group (second), the activity of MPO (0.56 ± 0.12) was markedly increased by 76.1% (0.10 ± 0.03) compared with that of the −ve group I. In contrast, the GOE treatment (group IV) had significantly lower MPO by 67.8% (0.18 ± 0.05) compared to that of group II. MPO activity showed a nonmarked change in other groups.

Impacts of GOE on LPS Phosphorylation Status Using PTK. The effects of GOE on the hepatic PTK level in (lung) in the LPS-treated mice group (second) are shown in Figure 7. The PTK levels in the lung were markedly increased in the second group (LPS) by 50.1% compared to group I (18.30 ± 3.26 vs 36.70 ± 7.33, *, $p < 0.001$). Administration of GOE in group III reduced markedly in PTK by 44.4% compared to that in group II (induction group) (20.39 ± 2.13 vs 36.70 ± 7.33;

https://doi.org/10.1021/acsomega.3c03480
ACS Omega 2023, 8, 37971−37990

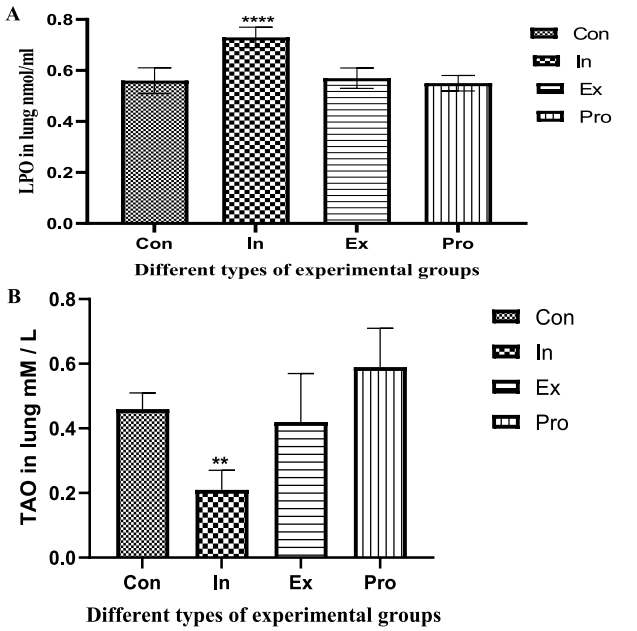

Figure 6. (A) Effect of GOE on the lung LPO level. (B) Total antioxidant biomarker activities (TAOs).

*, $p < 0.001$). The administration of GOE alone in group IV (+ve control group) resulted in a nonsignificant decrease in the PTK levels from 18.30 ± 3.26 to 17.51 ± 3.48. The values of PTK activities showed a nonmarked change in other groups.

Effect of GOE on LPS-Induced Histopathology. Under a light microscope, the lung tissues from the control group showed a normal structure. No histological alterations were observed (Figure 8). However, GOE dramatically reduced the extent of pathogenic alterations brought on by LPS (Figure 8). However, compared to the GOE group, LPS severely damaged the lungs' histological alterations (Figure 8). The scores for histological lung damage are shown in Figure 8. GOE had varied inflammatory effects on the lung tissue of mice exposed to LPS. Mice from the control, LPS, and LPS + GOE groups were used to study representative lung histological changes. H&E staining was used to detect pathological alterations in lung tissues (light microscopy, 200X); more details about Figure 8 are described in the Supporting Information.

Effect of GOE on Expression of TNF-α against LPS. The current study revealed that LPS markedly elevated the synthesis and expression of the inflammatory cytokine TNF-α (Figure 9) compared to the control group treated with GOE. A 200 mg/kg amount significantly diminished both inflammatory cytokine parameters compared to the LPS group (Figure 9). Interestingly, GOE at 200 mg/kg doses significantly modulated the reduction in TNF-α and expression levels in the tissue compared to the LPS group. More detail is described in Figure 9 in the Supporting Information.

Docking Study Results. Results of the docking experiments of 4DN5 (NF-κB) have significant effects that ensure that the best-docked poses of the lead compounds are aligned with catechol, chlorogenic acids, gallic acid, hydroquinone, kaempferol, and rosmarinic acid, with target protein with affinity values of −5, −6.8, −6.1, −4.9, −9.8, and −8.3 kcal/mol, respectively, which indicate experiment validity, showing the superior activities of kaempferol and rosmarinic acid with free binding energies equal to −9.8 and −8.3 kcal/mol, respectively. The establishment of five types of contacts, conventional hydrogen bonds (LEU A:472, SER A:476, LYS A:429), π-anion (ASP A:534), π-sulfur (CYS A:533), π-σ (VAL A:414), and π-alkyl (ALA A:427, LEU A:406, LEU A:522), with the active site residues (amino acids) might explain the solid binding of rosmarinic acid to the active site of 4DN5. For example, kaempferol's strong binding at the active site of 4DN5 might be explained by the formation of four

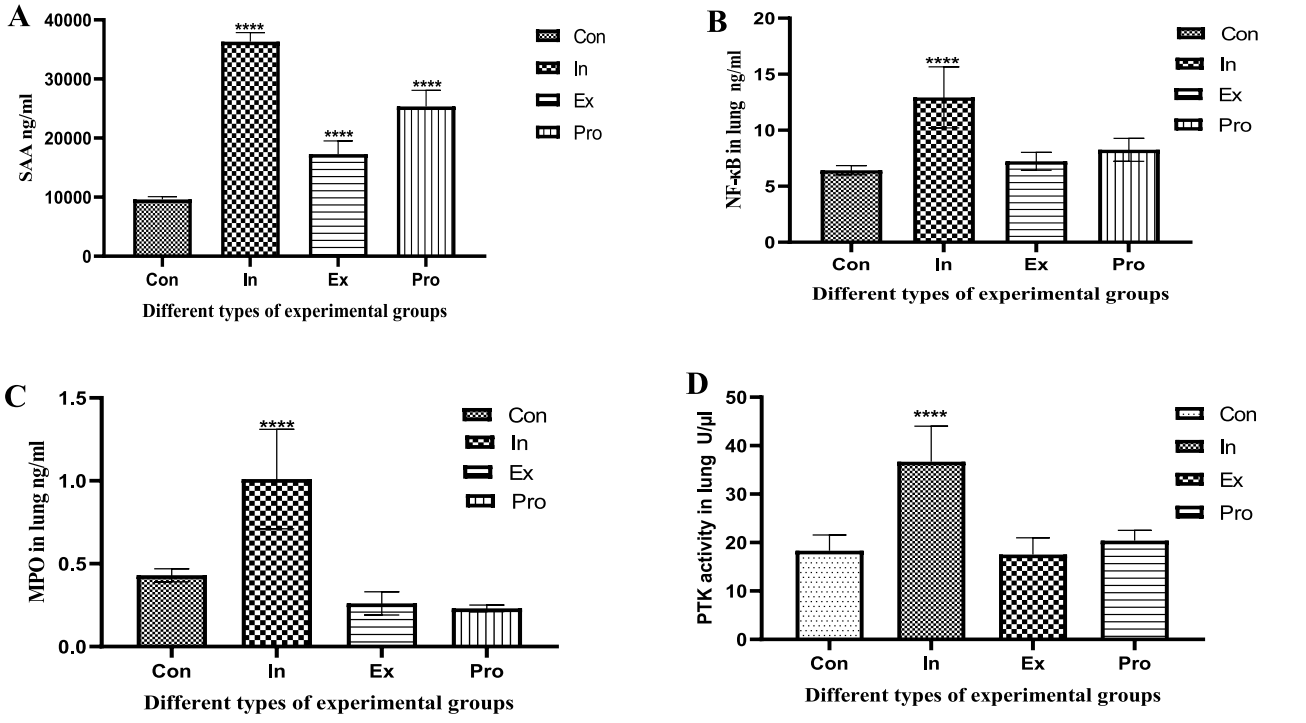

Figure 7. Effects of GOE on SAA (A), NF-κB (B), and MPO (C) inflammatory biomarkers in mouse lungs and on (D) PTK in lungs.

https://doi.org/10.1021/acsomega.3c03480
ACS Omega 2023, 8, 37971−37990

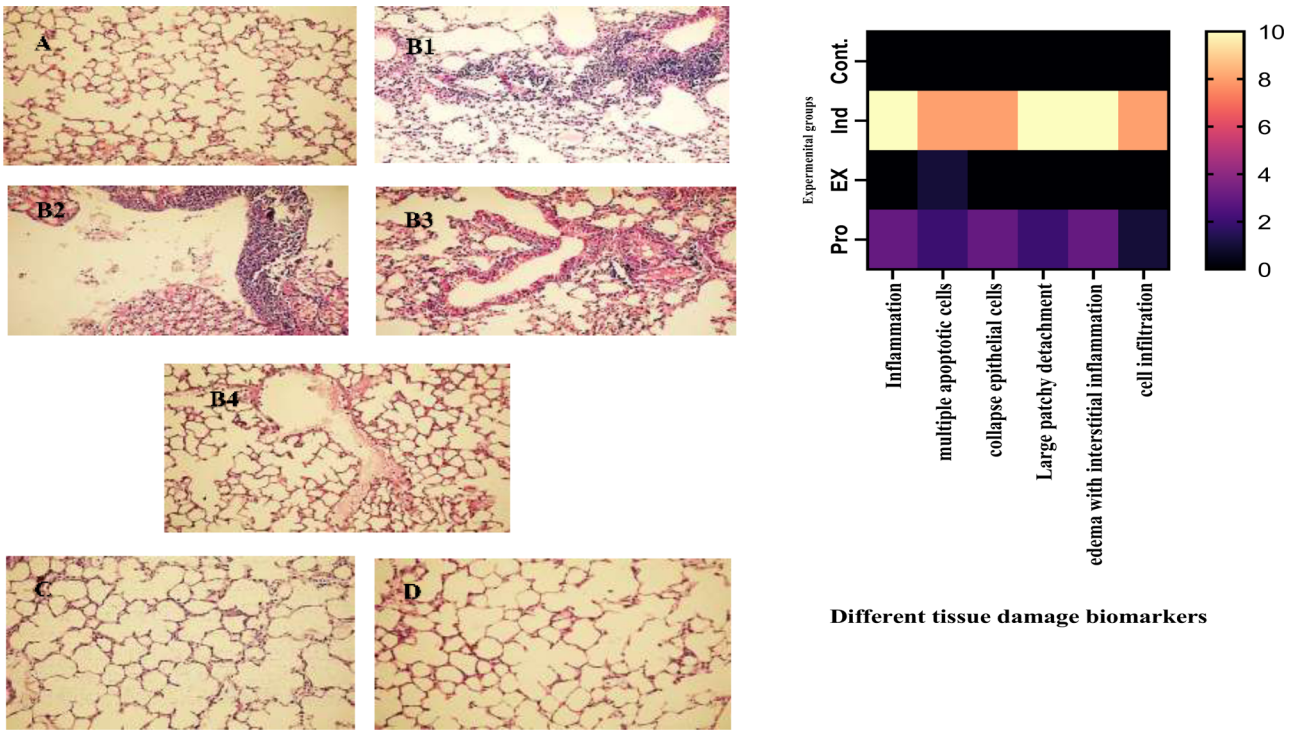

Figure 8. Impacts of GOE on alleviating LPS-induced histopathological changes in the lungs. (A) Control, (B) induction, (C) extraction, and (D) protection.

contacts, conventional hydrogen bonds (LYS A:429, ASP A:519, ASP A:534, LEU A:472), π-σ (VAL A:414, LEU A:522), π-sulfur (MET A:469), and π-alkyl (ALA A:427, LEU A:406, CYS A:533), as shown in Figure 10A).

Results of the docking experiments of 6MC1 (MAPK) have significant results that ensure that the best-docked poses of the lead compounds are aligned with catechol, chlorogenic acids, gallic acid, hydroquinone, kaempferol, and rosmarinic acid, with the target protein with affinity values of −5, −5.6, −5.6, −4.8, −7.7, and −7.2 kcal/mol, respectively, which indicate experiment validity, showing the superior activity of kaempferol and rosmarinic acid with free binding energies equal to −7.7 and −7.2 kcal/mol, respectively. The establishment of three types of contacts, conventional hydrogen bond (ASN A:448, THR A:417), π-stacked (TYR A:435), and π-alkyl (MET A:452, MET A:431, ILE A:420) contacts with the active site residues (amino acids) might explain the solid binding of rosmarinic acid to the active site of 6MC1 (MAPK). For, Kaempferol's strong binding at the active site of 6MC1 (MAPK) might be explained by the formation of 8 conventional hydrogen bonds THR A:417, carbon hydrogen bond MET A:452, TYR A:435, π-donor hydrogen bond MET A:452, TYR A:435, π-σ PRO A:447, π-sulfur MET A:452, π-π-stacked SER A:446, amide-π-stacked (TYR A:435), π-alkyl (MET A:452), as shown in Figure 10B.

Results of the docking experiments of 6NPY (NLRP3) have significant results that ensure that the best-docked poses of the lead compounds are aligned with catechol, chlorogenic acids, gallic acid, hydroquinone, kaempferol, and rosmarinic acid, with the target protein with affinity values of −4.9, −8.7, −6.1, −5.3, −8.5, and −8.9 kcal/mol, respectively, which indicate the experiment validity, showing superior activity to kaempferol and rosmarinic acid with free binding energies equal to −7.7 and −7.2 kcal/mol, respectively. The establishment of three types of conventional hydrogen bond (ASN A:448, THR A:417), π-stacked (TYR A:435), π-alky with the active site residues (amino acids), might explain the solid binding of rosmarinic acid to the active site of 6MC1 (MAPK). Kaempferol's strong binding at the active site of 6MC1 (MAPK) might be explained by the formation of five conventional hydrogen bonds THR A:167, ARG A:165, carbon hydrogen bond (MET A:452, TYR A:435), π-donor hydrogen bond ILE A:232, TTRP A:414), π-σ ILE A:232, π-π-stacked TRP A:414, π-alkyl PRO A:410, as shown in Figure 10C).

Results of the docking experiments of 7KP9 (TNF-α) have significant results that ensure that the best-docked poses of the lead compounds are aligned with catechol, chlorogenic acids, gallic acid, hydroquinone, kaempferol, and rosmarinic acid, with the target protein with affinity values of −4.1, −6.2, −4.9, −3.8, −6.4, and −6.1 kcal/mol, respectively, which indicate the experiment validity, showing superior activity to kaempferol and chlorogenic acids with free binding energies equal to −6.4 and −6.2 kcal/mol, respectively. The establishment of 3 types of conventional hydrogen bond (GLN C:47, ASN C:46), π-anion (GLU C:135), and π-alkyl (PRO C:139) contacts with the active site residues (amino acids) might explain the solid binding of kaempferol to the active site of 7KP9 (TNF-α). Chlorogenic acids' strong binding at the active site of 7KP9 (TNF-α) might be explained by forming 3 conventional hydrogen bonds THR C:77, THR C:79, LEU C:26, ASN C:46 and π-donor hydrogen bond LEU C:26 and π-alkyl, as shown in Figures 10D and Table 2.

DISCUSSION

Both lung and brain diseases are strongly induced by the LPS model. Besides use in lung studies, LPS is also useful for studying neuroinflammation in neurodegenerative diseases. It

https://doi.org/10.1021/acsomega.3c03480
ACS Omega 2023, 8, 37971−37990

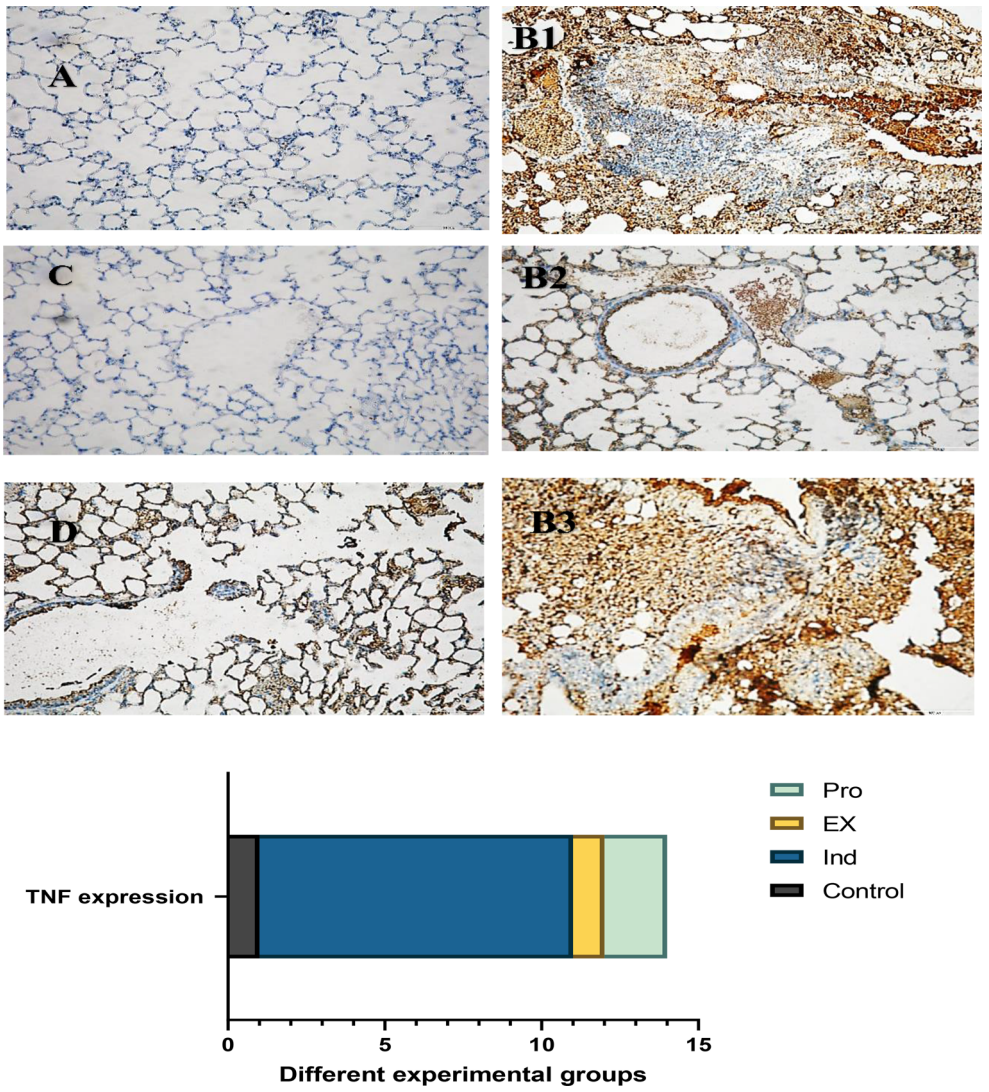

Figure 9. Impacts of GOE in alleviating the expression of TNF-α against LPS-induced immuno-histochemistry changes in the lungs. (A) Control, (B) induction, (C) extraction, and (D) protection.

is widespread to use LPS in vivo as well as in vitro. The CNS and peripheral nervous systems can be stimulated by single or multiple injections of this compound. Several fundamental connections exist between the brain and lungs. A vicious cycle is triggered when the brain−lung interaction is seriously compromised in patients with traumatic brain injury. Although the mechanisms of the interaction are not fully understood, several hypotheses, namely, the "blast injury" theory or "double hit" model, have been proposed, forming the basis of its development and progression.[23] In addition to communicating between the brain and the lungs, the lungs communicate with the brain via complex pathways. Among pulmonary disorders accompanying brain injuries, neurogenic pulmonary edema, acute respiratory distress syndrome, and ventilator-associated pneumonia are the most common, while hypoxia in the brain and intracranial hypertension are the most common brain disorders following lung injuries.[24]

A higher concentration of oxygen and reactive oxygen is contained within the lungs, making them the first frontier between the entry of oxygen and its delivery to the mitochondria.[25] Disruption of normal oxidative balance has been reported to be significant in the progression of the inflammatory response in several lung diseases caused by infection pathogenesis; there are many examples, such as ALI, acute ARDS, and COPD.[26] COVID-19 infection and the complications of those infections, resulting in ALI and/or ARDS, are also a severe problem that is an emerging target for developing new drug entities with little or no side effects.[27] Administration or exposure to LPS causes various symptoms, such as in patients with ALI, ARDS, and sepsis, and also increases the risk for Alzheimer's disease.[28] The development of such exposure causes a pro-inflammatory response in cells, hepatocytes, and Kupffer cells. NF-κB is a severe inflammatory cytokine and is a biomarker for several diseases, such as respiratory and Alzheimer's diseases; LPS induces the expression and locations of NF-κB.[29] The maximum immune response peak of the NF-κB serum was reported as early as 0.5−2 h after LPS injection.

In rodent animal models, the exposure of LPS induces NF-κB and ROS expression, which has been shown to stimulate NF-κB signaling through the classical IKK-structured pathway, to prompt infection to affect diverse organs, for example, the kidneys and liver, and to have a great effect on the brain also.[30] They investigated the LPS oxidative stress and the protecting

https://doi.org/10.1021/acsomega.3c03480
ACS Omega 2023, 8, 37971−37990

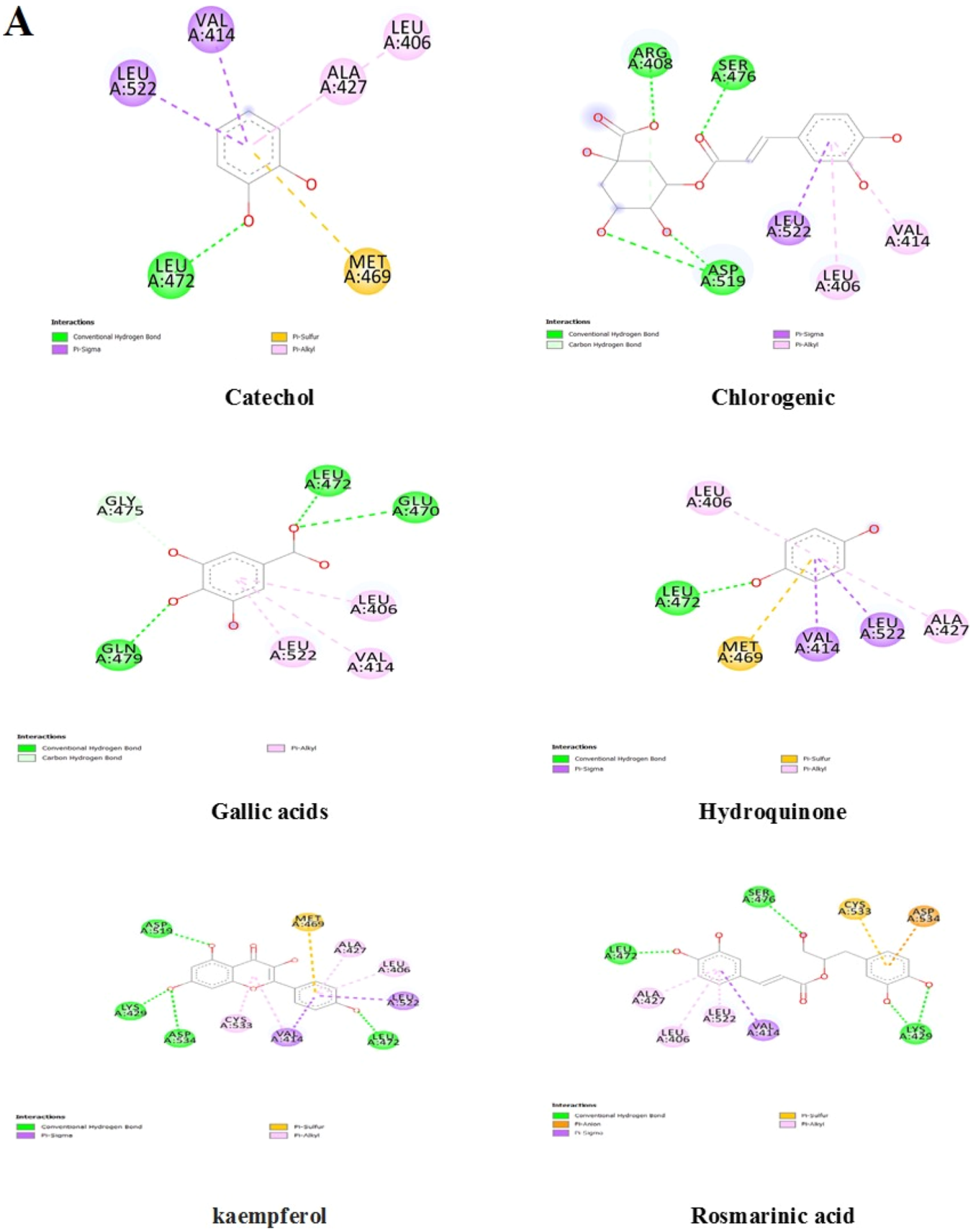

Figure 10. continued

https://doi.org/10.1021/acsomega.3c03480
ACS Omega 2023, 8, 37971−37990

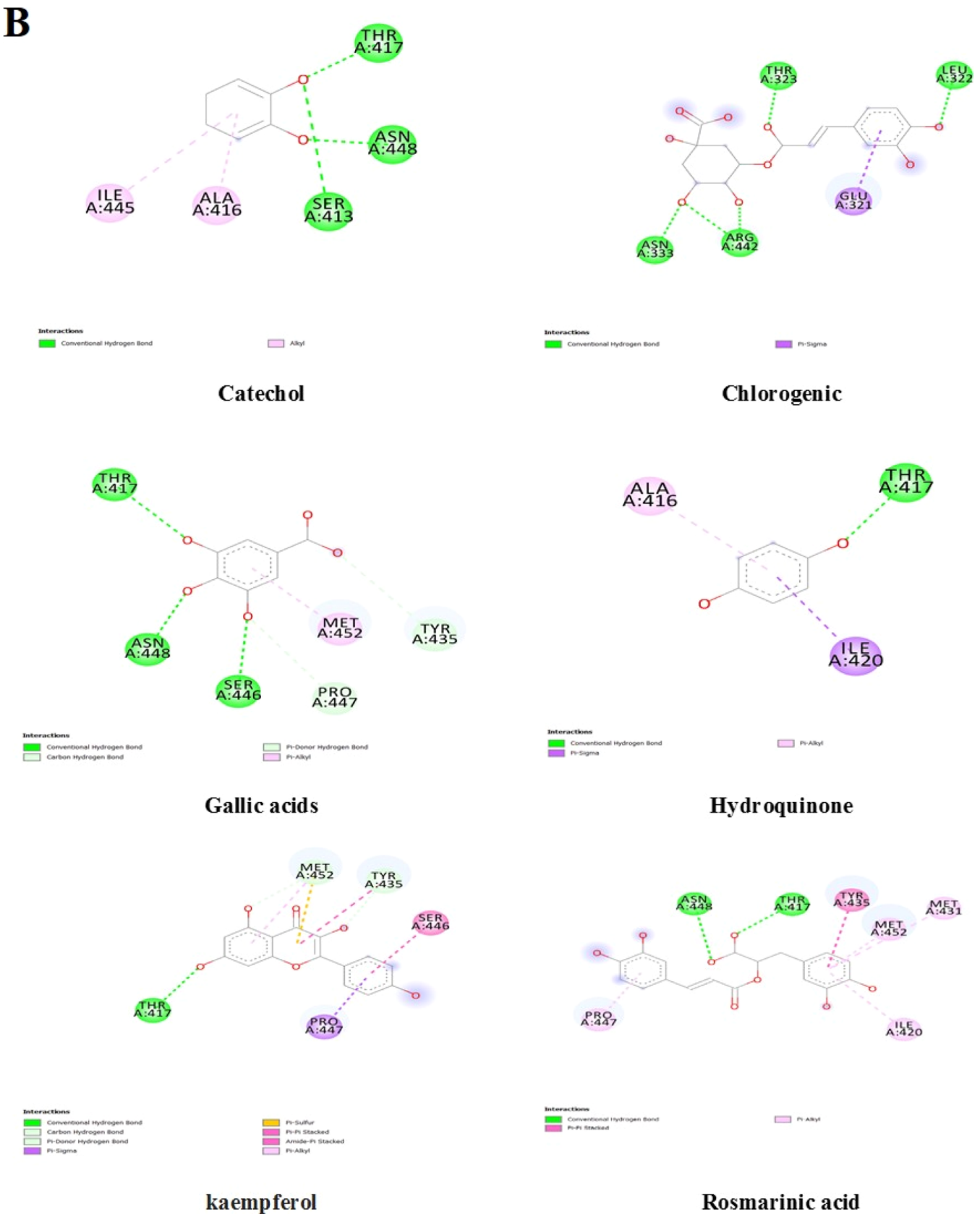

Figure 10. continued

https://doi.org/10.1021/acsomega.3c03480
ACS Omega 2023, 8, 37971−37990

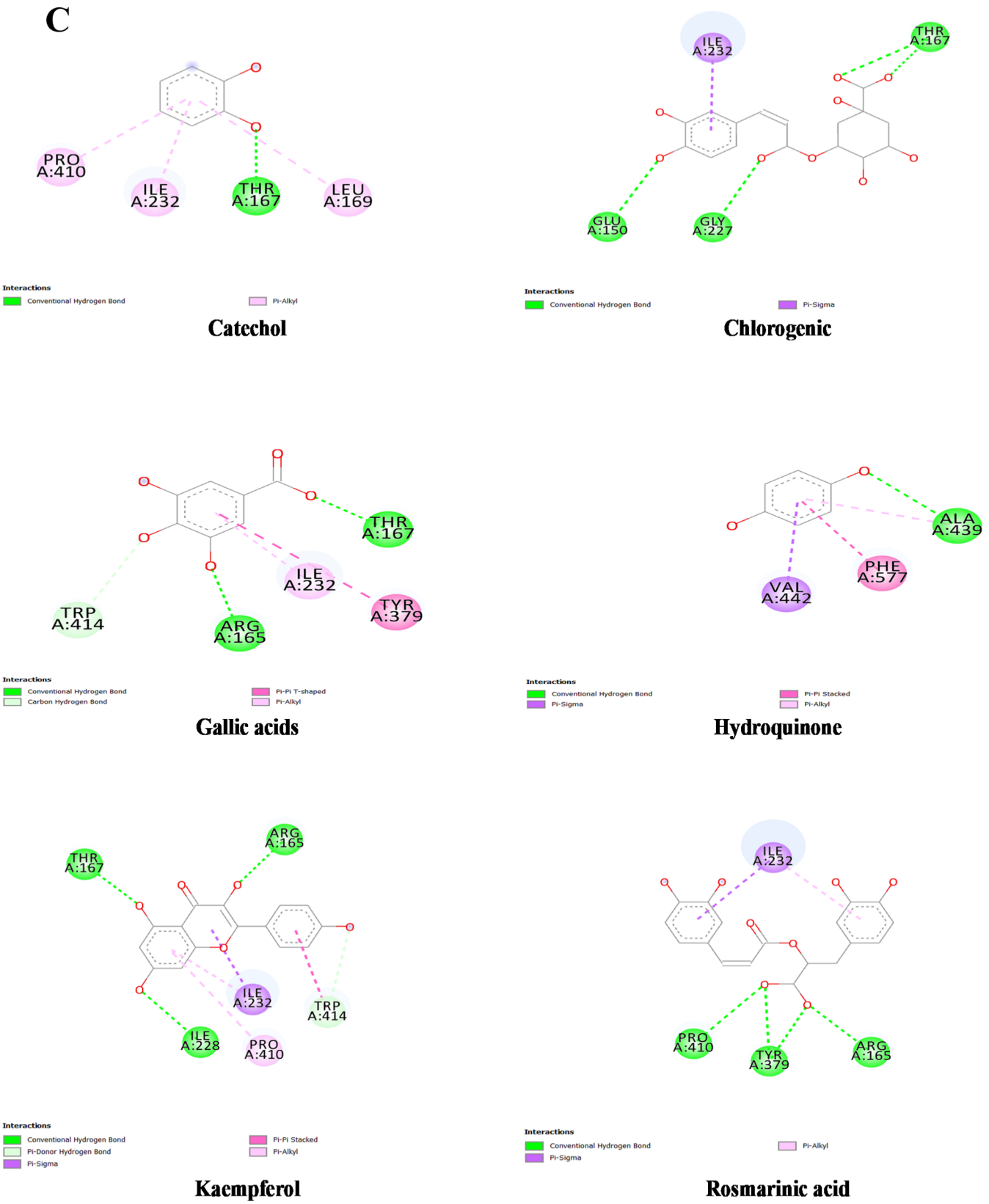

Figure 10. 2D structure of the different polyphenolic compounds against (A) 4DN5 (NF-κB), (B) 6MC1 (MAPK), (C) 6NPY (NLRP3), and (D) 7KP9 (TNF-α).

function of GOE. They revealed that GOE had an antioxidant impact on cytotoxicity raised by LPS by decreasing the extent of NF-κB expression and the level of different inflammatory biomarkers. Activation of NF-κB in the liver results in elevated levels of TNF-α, IL-1, and IL-6[31] expression. Marine organisms are a wealthy supply of anti-inflammatory, biologically bioactive lipids.[10−16,29] The current study confirmed the ability of GOE as a potent antioxidant and anti-inflammatory

https://doi.org/10.1021/acsomega.3c03480
ACS Omega 2023, 8, 37971−37990

Table 2. Affinity (kcal/mol) Score of Polyphenolic Compounds in GOE Extracts against Different Target Proteins

Compounds	4DN5 (NFKB)	Affinity (kcal/mol)	6MC1 (MAPK)	Affinity (kcal/mol)	6NPY (NLRP3)	Affinity (kcal/mol)	(7KP9) TNF	Affinity (kcal/mol)
Catechol	LEU 406	−5	SER 413	−5	THR 167	−4.9	VAL 17	−4.1
	VAL 414		ALA 416		LEU 169		GLN 149	
	ALA 427		THR 417		ILE 232		VAL 150	
	LEU 472		ILE 445		PRO 410			
	LEU 522		ASN 448					
Chlorogenic acids	LEU 406	−6.8	GLU 321	−5.6	GLU 150	−8.7	LEU 26	−6.2
	ARG 408		LEU 322		THR 167		ASN 46	
	VAL 414		THR 323		GLY 227		THR 77	
	SER 476		ASN 333		ILE 232		THR 79	
	ASP 519		ARG 442					
	LEU 522							
Gallic acid	LEU 406	−6.1	THR 417	−5.6	ARG 165	−6.1	THR 77	−4.9
	VAL 414		TYR 435		THR 167		THR 79	
	GLU 470		SER 446		ILE 232		SER 81	
	LEU 472		PRO 447		TYR 379		ASN 92	
	GLY 475		ASN 448		TRP 414		GLU 135	
	GLN 479		MET 452					
	LEU 522							
Hydroquinone	LEU 406	−4.9	ALA 416	−4.8	ALA 439	−5.3	THR 79	−3.8
	VAL 414		THR 417		VAL 442		SER 81	
	ALA 427		ILE 420		PHE 577		LYS 90	
	MET 469						ASN 92	
	LEU 472							
	LEU 522							
Kaempferol	LEU 406	−9.8	THR 417	−7.7	ARG 165	−8.5	ASN 46	−6.4
	VAL 414		TYR 435		THR 167		GLN 47	
	ALA 427		SER 446		ILE 228		GLU 135	
	LYS 429		PRO 447		ILE 232		PRO 139	
	MET 469		MET 452		PRO 410			
	LEU 472		TRP 414					
	ASP 519							
	LEU 522							
	CYS 533							
	ASP 534							
Rosmarinic acid	LEU 406	−8.3	UNK 0	−7.2	UNK 0	−8.9	UNK 0	−6.1
	VAL 414		THR 417		ARG 165		HIS 15	
	ALA 427		ILE 420		ILE 232		TYR 59	
	LYS 429		MET 431		TYR 379		GLN 61	
	LEU 472		TYR 435		PRO 410		LEU 120	
	SER 476		PRO 447				GLY 121	
	LEU 522		ASN 448					
	CYS 533		MET 452					
	ASP 534							

agent. It examined the bioactive secondary metabolite contents of polyphenolic compounds and fatty acids through an investigation for anti-inflammatory by inhibiting the manufacturing of NO, ACHI, (TNF-α) in LPS-induced lung mouse tissues.[31] GOE revealed the presence of excessive quantities of fatty acids that notably inhibit the synthesis of NO and TNF-α, which agrees with previous studies that confirmed red algae's ability against TNF-α and NO.[32] Marine algae comprise a large variety of extraordinarily energetic bioactive compounds, especially anti-inflammatory compounds, that also have been seen in GOE; the current study confirmed the presence of a variety of bioactive molecules, along with phenolics, flavonoids, tannins, carotenoids, and sulfated polysaccharide total contents, and discovered the existence of plenty of those compounds. Various huge biochemical and pharmaceutical applications have been reported for red algae due to their antioxidant capacity and anti-inflammatory as well as anticancer properties, which proposed GOE as a strong candidate for antioxidant, anti-inflammatory, and anticancer drugs.[33,34] Fatty acids are an essential bioactive anti-inflammatory compound consisting of omega-3 polyunsaturated fatty acids (n-3 PUFAs); hence, their extracts may be potent as nutritional substances in chronic metabolic diseases such as inflammatory diseases and Alzheimer's. These compounds were notably examined for their activity as an anticancer against different cancerous cell lines.[18−22] However, there is no prior study concerning the effect of red algae, specifically GOE.

Against acute lung injury as a possible drug candidate (protect, prevent, and treat), LPS induced ALI and its possible pathways. The study confirmed that GOE possesses an effective protecting agent against LPS destructive effects. It

https://doi.org/10.1021/acsomega.3c03480
ACS Omega 2023, 8, 37971−37990

substantially reduced pulmonary edema because of vastly lower lung pathological LPS harmful effects. Also, GOE inhibited and suppressed inflammation infiltration by LPS into the lung tissue and attenuated myeloperoxidase in the lung[34] (Figure 10C).

GOE significantly improved the histopathological lesions induced by LPS.[35] Pretreatment with GOE decreases markedly the oxidative stress induced by LPS and increases tissue's total antioxidant capacity (lung; Figure 6). The role of GOE as an anti-inflammatory against LPS-induced ALI, was evident through the attenuation of pro-inflammatory cytokine levels, i.e., TNF -α and IL-6, NF-κB. Likewise, GOE inhibited the LPS-induced increase of pro-apoptotic proteins Bax and caspase-3. Collectively, GOE exerted protective activity against ALI induced by LPS via antioxidant, anti-inflammatory, and anti-apoptotic pathways[36] According to recent studies, people with chronic inflammatory illnesses are more inclined to look for natural anti-inflammatory drugs to reduce the adverse effects of using steroids and NSAIDs for an extended time. Therefore, creating novel, safer anti-inflammatory nutraceuticals is clinically relevant and may greatly impact treating inflammatory responses. Marine extracts and functional foods are comparatively undiscovered sources of potential anti-inflammatory compounds.[37] Different polyphenolic compounds were found in the extracts, such as chlorogenic acid, one of the world's most abundant polyphenols. Accumulated evidence has shown that chlorogenic acid possesses multiple biological activities, including antibacterial, antioxidant, anti-Alzheimer's, and anticarcinogenic. Chlorogenic acid inhibits the production of staphylococcal exotoxins IL1β, TNFα, IL6, interferon (INFγ), MCP l, PIMlα, and MIPlβ in human peripheral blood mononuclear cells.[38]

Moreover, Shan et al.[39] found that chlorogenic acid regulates inflammation cytokines in LPS-activated macrophages. Studies suggest that chlorogenic acid plays a role in the pathogenesis of autoimmune disorders. LPS-induced lung injury has been linked to inflammatory cytokines, and chlorogenic acid may also have anti-inflammatory properties useful in treating ALI and ASDR. Several mediators mediate the inflammation caused by lung injury, but TNF-α plays a key role.[40] It has been reported that TNF-α is a highly pro-inflammatory cytokine initiator of inflammatory reactions and induces apoptosis of the lung.[41] Previous research had proven that injection of chlorogenic acid before LPS assignment notably inhibited the transcriptional expression of TNF-α, which will be partly responsible for the protecting consequences of chlorogenic acid.

Further research has shown that chlorogenic acid affects TLR4, one of the TLR proteins, and is essential in the LPS-mediated signaling process.[42] Treatment with chlorogenic acid inhibited the transcription of TLR4 to the basal level, which could result in the inhibition of LPS-induced NF-κB activity (Figure 7B). Previously, this was found to be true. The results suggest chlorogenic acid reduces inflammation by reducing each NF-κB downstream signaling pathway mRNA expression and phosphorylation. Figure 7D shows that total protein tyrosine kinase activity decreased in the current study.[43]

Rosmarinic acids (RAs) also possess comparable anti-inflammatory and antioxidant effects. Many pathophysiological pathways contribute to inflammation, but the interaction of RAs with the complementary system has the most notable effect on infection. RA blocks complement activation by interacting covalently with the active complement element C3b at the infection site.[44] According to Scheckel et al.,[45] RA may be a potent inhibitor of the pro-inflammatory gene COX2, which is supported by the current study's finding that GOE in vitro analysis of COX1 and COX2 revealed strong anti-COX1 and -COX2 activity.[33]

As a result of oxygen−glucose deprivation, RA inhibits apoptosis and cytotoxicity.[33] In an experimental rat model of sepsis, Luo et al.[46] studied the effects of RA on cultured RAW264.7 cells. The RA reduced inflammation caused by LPS in RAW264.7 cells by activating TNF-α, IL-6, and high-mobility group protein 1. This suggests that the antiseptic properties of RA are mediated by a reduction in inflammatory mediators, both locally and systemically. According to a recent study, hemodialysis fluid is supplemented with RA, reduces inflammation, and is biocompatible. By supplementing HUVECs with RA, researchers found that LPS-induced nitric oxide production decreased and nitric oxide synthase expression was downregulated. RA reduces pro-inflammatory mediator production in HUVECs by Wang et al.[47] RA was studied for its antiviral properties. The antiviral effects of RA have shown a significant decrease in mortality rates in mice infected with the Japanese encephalitis virus. A significant difference between inflamed RA-handled animals and non-treated inflamed animals regarding viral virulence and pro-inflammatory cytokines was observed. It is widely known that kaempferol (KF) has bioactive properties. It is an important natural flavonoid aglycone, especially in fruits and vegetables. In molecular survival and apoptosis, protein kinase B (PKB), also known as AKT, plays an important role. As a result of treatment, PI3K was inhibited and Akt phosphorylated in K562 and U937 cells. Cells treated with KF de-phosphorylate Akt at Ser 473 and Thr 308.[48]

Activation of caspase-3, caspase-7, caspase-9, and PARP occurs when KF is present. In addition, KF inhibits PI3K and AKT phosphorylation triggered by LPS and ATP in cardiac fibroblasts, protecting them from inflammation.[48] In response to LPS, KF and its glycosides can also significantly reduce NO and TNF-α production in RAW 264.7 cells. They also inhibit the nuclear translocation of NF-κB and p65, which are inhibited by TNF-α and interleukin-1 (IL-1). In response to GA, caspase-3 and -9 are expressed, Bcl-2/Bax ratios are altered, tyrosine phosphorylation via BCR/ALB kinase is inhibited, and COX2 is decreased. Figure 4C shows that GA inhibits COX1 and COX2 activity, indicating its anti-inflammatory properties. The increased expression of COX2 causes most cancer cases to progress by triggering cell division and inhibiting apoptosis.[49,50] Because of its role in gene expression, it is important in treating inflammatory conditions. Maximum anti-inflammatory capsules inhibit pro-inflammatory cytokines by inhibiting the activation of NF-B.[51] Several reports found that selective inhibitors inhibit the production of NOS, COX2, TNF-α, and IL-1. NF-κB-structured p65 acetylation and inflammatory markers are inhibited by GA, according to Desai et al.[52] Additionally, acetylation of p65 stimulates transcription activation, DNA binding, and binding of IBB to DNA. It is well established that the low acetylation price of p65 results in the complete absence of NF-B characteristics, indicating that acetylation is vital for NF-κB-mediated signaling.[53]

When included in a proper diet, polyunsaturated fatty acids (PUFAs) may also have numerous beneficial fitness effects compared to saturated fats.[54] Since the human body cannot synthesize PUFAs bigger than 18 carbons, it relies on meals for

https://doi.org/10.1021/acsomega.3c03480
ACS Omega 2023, 8, 37971−37990

long-chain PUFAs. Marine lipids are the main source of biologically active PUFAs, omega-3, α-linolenic, and omega-6 linoleic PUFAs (Figure 3). These have shown that PUFAs reduce chronic inflammation, cancer, cardiovascular disease, and so on. This is accomplished by using substances that compete with arachidonic acid or indirectly affect transcription factors or nuclear receptors, which are important for inflammatory genes.[55,56] Nutritional PUFAs have been important in preventing persistent inflammatory diseases, such as arthritis, bronchial allergies, and neuroinflammatory diseases. Because of the amount and type of eicosanoids they produce, docosahexaenoic acid (DHA; C22:6) and eicosatetraenoic acid (C20:5) play crucial roles in infection. Huerta-Yépez et al.[57] report that this interaction impairs intracellular signaling pathways, transcription factors, and gene expression mechanisms. There is convincing evidence that DHA migrates into and protects against stages of pro-inflammatory cytokines (IL-1β, IL-6, and TNF-α). Moreover, numerous fitness problems, which include extended inflammatory processes, poor fetal development, and high-risk factors for Alzheimer's disease, have been related to low eicosapentaenoic acid and DHA PUFA diets.[58] The bioactive polyphenol chlorogenic acid possesses a high level of biological activity.

For example, chlorogenic acids (CA.) has a wide variety of biologically active properties, including antibacterial, antioxidant, and anticarcinogenic properties.[59] As Naeed et al.,[60] demonstrated, CA. inhibits the biosynthesis of interferons (INFs; IL-1, TNF -α), IL-6, and interferons caused by staphylococcal exotoxins. It also regulates the expression of inflammatory cytokines in macrophages activated by LPS. An LPS-binding protein called SAA limits the pro-inflammatory effects of LPS in mice with acute lung injury. Several inflammatory factors have been recently used as biomarkers, including SAA and CRP.[61] Moreover, they can serve as biomarkers during the pathogenesis of COVID-19 and estimate the degree of illness. In terms of host immunity and protection, SAA's role is unclear. Even though its structure differs from chemokines and other common chemoattractants like C5a, it has been shown to attract monocytes, lymphocytes, and granulocytes.[62] SAA causes various leukocytes to release cytokines, including IL-1, IL-6, and TNF-α, according to in vitro study.[63] Due to its acute-phase role as a mediator of the local effector Th17 reaction stimulated by the intestinal microbiome, SAA was cautiously tested for its cytokine-like activity, tissue expression profile, signaling properties, and in vivo capabilities in host protection and infection.[40,64] As a protein with multiple functions, SAA may be associated with neurodegenerative diseases such as Parkinson's disease. In addition to its role in inflammation, tumorigenesis, skin homeostasis, and accumulation as misfolded AA-amyloid proteins, SAA also contributes to immunity. In patients suffering from lung cancer and obstructive and restrictive lung diseases (COPD, connective tissue lung diseases, and sarcoidosis), SAA levels were measured in their biological fluids. A traumatic brain injury results in the liver producing a high level of SAA protein. An accurate and direct measurement of the severity of traumatic brain injury can be made using liver protein levels when pathological symptoms or neuroimaging analysis are not able to provide this information.[65,66] In simulated physiological conditions, all plasma lipoprotein subclasses of LPS sequester in HDL, as HDL binds LPS very strongly and redistributes it to LDL and VLDL. While the process and outcome of LPS binding to LDL and VLDL are unknown, HDL appears to be the first line of defense against persistent LPS cell immunity.[67]

The immune-stimulatory action of LPS is reduced when Gram-negative bacteria are infected by binding and translocation to certain lipoproteins. HDL is the number one endotoxin-scavenging lipoprotein in blood or plasma (ex vivo), and a time-dependent transfer of HDL-related LPS to LDL and VLDL has been established.[68]

As a result of adipose tissue lipolysis, plasma or serum triglyceride levels increased, resulting in increased de novo synthesis of hepatic fat and reduction in the level of fatty acid oxidation. As a result of reduced lipoprotein lipase and apo E levels in VLDL, the clearance of VLDL decreases with severe infection. Increasing hepatic LDL cholesterol synthesis and reduced LDL clearance, conversion to bile acids, and secretion of LDL cholesterol cause hypercholesterolemia in rodents. Various adjustments in proteins essential to HDL metabolism result in an increase in the transport of LDL cholesterol to immune cells and a reduction in opposite LDL cholesterol delivery.[69]

LDL and VLDL oxidation will rise even though HDL is a pro-inflammatory molecule. Sphingomyelin, ceramide, and glucosylceramide are added to lipoproteins to enhance their absorption by macrophages. At some time during the infection, early and ongoing metabolic alterations raise blood triglyceride (TG) levels, which are characterized by an increase in very low density lipoprotein (VLDL) levels. Through a variety of mechanisms, including many cytokines, the APR period causes hypertriglyceridemia. Whether the rise in glucocorticoid levels during infection significantly influences lipid metabolism is unclear.[70] Previous studies have shown that Gram-positive or Gram-negative bacterial illnesses and viral infections raise serum TG levels. Hypertriglyceridemia is caused by either an infection with Gram-negative germs or by Gram-positive microorganisms' lipoteichoic acid (LTA) molecular wall component.[71] Within 2 h of injection, the effect of LPS on cytokines and lipids causes an increase in several cytokines in serum TG levels and hypertriglyceridemia, which is maintained for at least 24 h. The doses of LPS or cytokines that cause hypertriglyceridemia in rodents are similar to those that cause anorexia and fever and alter acute-phase protein synthesis, indicating that hypertriglyceridemia is an entirely physiological and sensitive aspect of the host's response to infection rather than a sign of toxicity.[72] Increased VLDL results from either better VLDL synthesis or decreased VLDL clearance, depending on the dosage of LPS. Due to increased hepatic fatty acid (FA) synthesis, adipose tissue lipolysis, and suppression of FA oxidation and ketogenesis, VLDL synthesis will rise at low dosages.[73]

Research has focused primarily on the NLRP3 inflammasome, a sensor molecule. When the homeostatic state of a cell is disturbed, the stress sensor NLRP3 picks it up. The traditional inflammasome activation and noncanonical pathways are viable options for NLRP3 activation. It takes two distinct and concurrent processes, priming (transcription) and activation, to set off the NLRP3 inflammasome (oligomerization). Step one involves innate immune signaling via the TLR-adaptor protein MyD88 and/or cytokine receptors like the tumor necrosis factor (TNF-α) receptor, which activates nuclear factor-B (NF-κB) and boosts pro-IL-1 and NLRP3 transcription. In the second step, the NLRP3 inflammasome oligomerizes and activates caspase-1, processing and releasing IL-1 and IL-18. It has been found that many polyphenols can

https://doi.org/10.1021/acsomega.3c03480
ACS Omega 2023, 8, 37971−37990

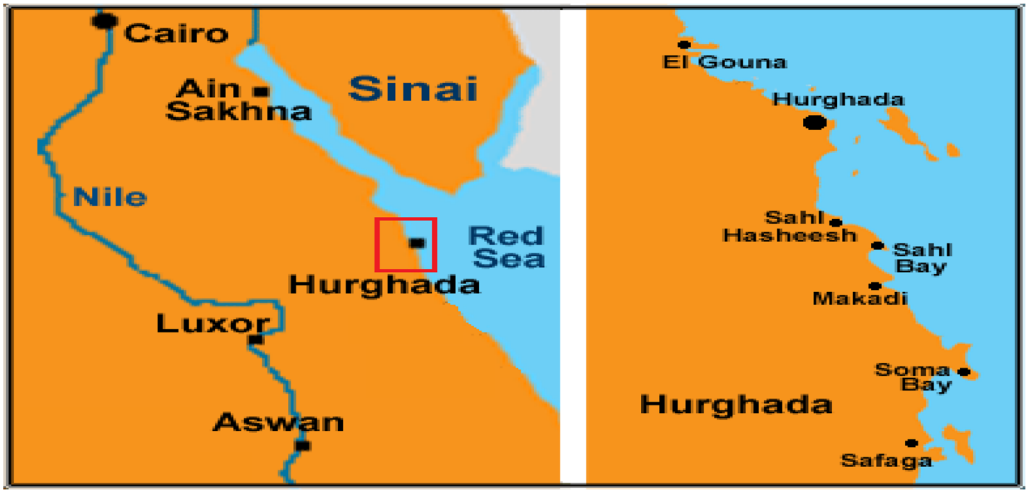

Figure 11. Location of the sampling area at Hurghada on the Egyptian Red Sea coast.

ameliorate CNS diseases by blocking the critical TRL-MyD88-NF-κB pathway of NLRP3 inflammasome activation. Previous studies have shown that polyphenolic therapy effectively promotes antiaging, pro-anti-inflammatory, antioxidant, and anti-apoptotic effects by inhibiting NF-κB/NLRP3 signaling. Evidence shows polyphenols stimulate the anti-inflammatory AMPK, Sirt1, and PPAR-γ pathways (PGC-1).[74]

Several diseases are reported to be connected to the NLRP3 inflammasome, for example, diabetes, cardiovascular disease, neurodegenerative, and atherosclerosis, prompting therapeutic interest in NLRP3 inflammasome inhibitors. Several studies have validated many inhibitors of the NLRP3 inflammasome signal pathway.[75] Some of these inhibitors target NLRP3; direct targeting of NLRP3 prevents off-target immunosuppressive effects and limits tissue death. Polyphenolics are one of the most promising inhibitors of NLRP3. The current study investigates in silco screening showing good affinity from catechol, chlorogenic acids, gallic acid, hydroquinone, kaempferol, and rosmarinic acid toward NLRP3, with rosmarinic acid and kaempferol having affinities −8.9 and −85 kcal/mol, respectively; the type of bond reveals the interactions between ligand and the target protein as shown in Figure 10.

This effect may aid in further reducing the NLRP3 activity. Polyphenols decrease the progression of inflammation by interfering with three distinct pathways: inflammatory, oxidative, and apoptotic. Polyphenols influenced inflammation through the MAPK pathway and were demonstrated in the current study as we observed high affinity of the MAPK with possible inhibitors effect according to the type of bone and residues of amino acids as shown in Table 2. The kaempferol and rosmarinic acid showed higher activity with affinities of 7.7 and 7.2 kcal/mol, respectively. They are also anti-inflammatory since they can inhibit pro-inflammatory signaling pathways such as NF-κB and MAPK stimulation. According to several studies, TNF-α, IL-1, and IL-6 are pro-inflammatory cytokines implicated in the modulation of the immune response in inflammatory diseases and are associated with inflammatory processes. Mitogen-activated protein kinases (MAPK) control the generation of pro-inflammatory cytokines that cause several joint inflammations and lead to stimulating the destruction process. The current study investigated the role of polyphenolics as promising natural inhibitors using in silco screening; the results of the docking studies for TNF-α and NF-κB are presented in Figure 10 and Table 2, showing that kaempferol and rosmarinic acid have higher affinities with −9.8 and −8.3 kcal/mol, respectively, for NF-κB. In comparison, for TNF-α, the catechol and rosmarinic acids have higher affinities with 6.2 and 6.4 kcal/mol, respectively.

CONCLUSION

As part of a search for a novel marine bioactive that can prevent inflammation in general and LPS, GOE extracts were evaluated by using various assays and techniques (in vitro, in vivo, and in silco). The present study demonstrated that GOE has a more significant inhibitory potential against biomarkers (inflammatory, cancer-related, viral, and oxidative). In addition, in vivo studies confirmed the results of the in vitro studies, as biochemical results showed great improvements in the extract group compared to the group induced by LPS. The present study improved the protection of GOE against lung and brain inflammation. Further studies should explore its other possible effects.

MATERIAL AND METHODS

Area of Study. The Red Sea has a unique geography. Almost entirely enclosed by land, the Red Sea is one of the world's most important marine biodiversity repositories (Figure 11).

Its biological variety is incredibly diverse, with more than 1000 invertebrate species and more than 1200 species of fish and coral reefs, mangroves, and seagrasses.[76−78] Hurghada is located along the western edge of the northern Red Sea and stretches for approximately 60 km along the Red Sea coast (Figure 11).

Seaweed's Collection. GOE samples were collected from Hurghada-Sheraton at latitude 27 11 37.5 and longitude 33 50 48.4 during spring 2019 (Figure 1) and transported in sterile polyethylene bags preserved in an icebox at 0 °C to the laboratory. The NIOF team carried out the identification of the sample.

Instruments. HPLC (Agilent), GC-MS (Thermo, USA), and multimode reader were used.

Chemicals and Solvents. All chemicals were purchased from Sigma-Aldrich.

https://doi.org/10.1021/acsomega.3c03480
ACS Omega 2023, 8, 37971−37990

GOE Extraction of Bioactive Compounds. The extraction of bioactive secondary metabolites from GOE was performed according to Nabil-Adam et al.[79]

Qualitative Determination of Phytochemical Bioactive Compounds. Total phytochemical screening of GOE assessed different bioactive classes (phenolic, flavonoids, and carotenoids) according to Nabil-Adam et al.[14−16]

Phytochemical Screening of GOE Using GC-MS. GC-ITQ-MS analyzed GOE according to the method described in Nabil-Adam et al.[14−16]

Identification of Phytocompounds. Identifying and interpreting the GC-MS mass spectra GOE compounds was carried out using the National Institute of Standard and Technology (NIST) database.[80]

HPLC Analysis for Polyphenolic Screening. The identification of the polyphenols profile of the GOE compounds using HPLC was performed according to Uddin et al.[81]

Total Antioxidant and Anti-Alzheimer's Assessment of GOE. DPPH and ABTS+ radical-scavenging assay of the GOE was carried out according to Amarowicz et al.[82] and Chakraborty and Paulraj et al.[83] The anti-Alzheimer's assessment of the GOE was investigated using inhibition of AChE by GOE by Moyo et al.[84]

Determination of Anticancer and Anti-inflammatory Assessment of GOE. We used Takara Cat. No. MK410 Tyrosine Kinase Assay Kit, nonradioactive, for the test. GOE's inhibitory activity against sphingosine kinase 1 was measured with a colorimetric Cayman sphingosine kinase 1 inhibitor screening kit. An Ovine COX (Cayman) screening kit was used for determining anti-inflammatory properties (cyclooxygenase inhibitory activity). TNF-α inhibitory activity of GOE was determined using the KOMA BIOTECH Inc. colorimetric kit.

Antiviral Activity of GOE. The antiviral activity of GOE using reverse transcriptase (RT) inhibitory activity was done with a Roche colorimetric kit according to Fonteh et al.,[85].

Experimental Animals. The Theodor Bilharz Institute in Egypt provided 40 BALB/C mice weighing 30 and 40 g for this study. A protocol for the study was approved by the Ethics Committee of Alexandria University's Faculty of Medicine in accordance with ARRIVE guidelines.

Experimental Design. The animals were assigned into four groups (10 mice in each group), and each group was placed in two cages as follows in Table 3.

The tissue samples were collected from each group of mice after being sacrificed at the end of each week of treatment, as described by Enkhmaa et al.[86] and Kumar et al.[87] Following sacrifice of the mice, Lee et al.[88] performed the histopathological examination of each lung mouse group.

Table 3. Different Groups of the GOE Experiment

Group	Treatment
Group I (control group)	Received saline solution with intraperitoneal (i.p.) application and was considered a negative group (control); for 1 week
Group II (induction group)	Received i.p. 5 [mg/(kg of body weight)]/day LPS and served as induction (inflammatory group)
Group III (extract group)	Received i.p. 200 (mg/kg)/day GOE and served as an extract group.
Group VI (protected)	Received i.p. GOE (200 mg/kg)was administered for 2 h before treatment with LPS+ algal extract and consider a protected group

Tissue Preparation. The lung tissues were weighed, washed free of the blood, and adhered to using cold saline. The preparation was performed according to Abdel El Moniem et al.[89−91] There were raw liver homogenates for malondialdehyde (MDA), total antioxidant capacity, MPO, and PTK.

Blood, Liver, and Kidney Assays. According to Reitman and Frankel,[92] AST was determined, the albumin levels were determined using the Doumas et al.[93] methods, total bilirubin levels were determined using the Walters and Gerade method,[94] and total proteins were determined using the Biuret reaction as described by Gornall et al.[95] Henry et al.[96] developed a method to determine creatinine levels. The modified Berthelot reaction described by Patton and Crouch[97] determined urea concentrations enzymatically. The methods of Zollner and Kirsch[98] were used to determine the lipid levels. This study determined triglycerides and cholesterol enzymatically using the Bucolo and David method[99] and Allain et al.[100]

Determination of Total Antioxidant Assay. According to Kovacevic et al.,[101] total antioxidant capacity was determined. The absorbances of blank (A) and sample A against water at 510 nm were determined.

Pro-inflammatory Biomarkers. *Myeloperoxidase (MPO).* The activity was performed according to Pulli et al.;[102] NF-kB and SAA were tested according to the method described in the commercial kit (Invitrogen, Camarillo, CA, USA).

Histology and Immuno-histochemistry Study. Based on Griffith and Farris,[103] we performed histopathological analysis of the lungs and, also by the technique of Wang et al.[104] For assessing TNF-α expression in lung tissue samples, this was used.

In Silico Screening Approach. Molecular docking drug screening of natural compounds and crystal structure using AutoDock Vina experiments four the main inflammatory proteins were induced due to LPS induction. The target proteins were NF-κB, MAPK, NLRP3, and TNF-α with ID. 4DN5, 6MC1, 6NPY, and 7Kp9, respectively.

Preparation of Target Protein for In Silco Study. The protein structure is the crystal structure of 4DN5, NF-kB-inducing kinase (NIK), 6MC1 (MAPK), and the structure of MAP kinase phosphatase 5. 7KP9, TNF-α, and the proteins were retrieved from the Protein Data Bank. Ligands were removed from the proteins using PyMol. InPyMol is saved in PDB format for docking analysis.[105]

Preparation of Polyphenolics Ligand for In Silco Study. 3D (polyphenolic) structures were retrieved from the ZINC database. Results from an HPLC examination of GOE extract were used to inform the selection of natural compounds; the zinc ID is listed in a table in the Supporting Information (S1).

ADME Analysis (Pharmacodynamics and Pharmacokinetics) of the Polyphenolics. An ADME study was carried out to assess the medicinal chemistry, pharmacokinetics, and drug-likeness of the found polyphenolic compounds. Lipinski's rule[106] of five was used to guide the analysis using the open-source server SwissADME.[107] This study excluded constituents in the database that satisfied fewer than three criteria from further analysis.

Autodocking Using Natural Polyphenolic Compounds against Different Inflammatory Biomarkers Proteins. The docking experiment software Auto Dock Vina 1.0 was used in

https://doi.org/10.1021/acsomega.3c03480
ACS Omega 2023, 8, 37971−37990

this investigation. Using Auto Dock Tools 1.5.6, the grid box that was used to pinpoint the active site in the protein pocket was produced. The autodocking settings for each protein are displayed in the Supporting Information Table S2. All of the program's other settings are left at their default values. PyMol pogroms and BIOVINA Discovery Studio Visualizer 4.0 were used to create visual representations of the docking data.[108] The Grid parameters of each protein are listed in supplementary data.

Statistical Analysis. An experiment's average and standard deviation (SD) are expressed as an average and standard deviation. Using Duncan's test, we performed the following analysis of variance: 0.05 was set as the significance level. GraphPad Prism 5 was used to create all graphs.

■ ASSOCIATED CONTENT

Supporting Information

The Supporting Information is available free of charge at https://pubs.acs.org/doi/10.1021/acsomega.3c03480.

Rationale of our work; (Table S1) different proteins with their docking parameters; (Table S2) ligands of the current study with their accession number from the zinc database; description of protein preparations; (Figure S1) heatmap of different polyphenolics with four proteins; (Table S3) ADME analysis for GOE different polyphenolic; pharmacodynamics, pharmacokinetics, and ADME; (Figure S2) correlation of different polyphenolics with four proteins; abbreviation list (PDF)

■ AUTHOR INFORMATION

Corresponding Author

Mohamed L. Ashour − *Department of Pharmacognosy, Faculty of Pharmacy, Ain-Shams University, Cairo 11566, Egypt; Department of Pharmaceutical Sciences, Pharmacy Program, Batterjee Medical College, Jeddah 21442, Saudi Arabia;* orcid.org/0000-0002-9270-6267; Email: ashour@pharma.asu.edu.eg

Authors

Asmaa Nabil-Adam − *Marine Biotechnology and Natural Products Laboratory, National Institute of Oceanography & Fisheries, Alexandria 21556, Egypt*

Mohamed Attia Shreadah − *Marine Biotechnology and Natural Products Laboratory, National Institute of Oceanography & Fisheries, Alexandria 21556, Egypt*

Complete contact information is available at: https://pubs.acs.org/10.1021/acsomega.3c03480

Notes

Discolsure: The Ethics Committee Faculty of Medicine Alexandria University confirmed and permitted this study with serial no. 0304927.

The authors declare no competing financial interest.

■ REFERENCES

(1) Zou, L.; Ruan, F.; Huang, M.; Liang, L.; Huang, H.; Hong, Z.; Yu, J.; Kang, M.; Song, Y.; Xia, J.; Guo, Q.; Song, T.; He, J.; Yen, H.-L.; Peiris, M.; Wu, J. SARS-CoV-2 Viral Load in Upper Respiratory Specimens of Infected Patients. *N Engl J. Med.* **2020**, *382* (12), 1177−1179.

(2) Sampath, V. P. Bacterial endotoxin-lipopolysaccharide; structure, function and its role in immunity in vertebrates and invertebrates. *Agric Nat. Resour.* **2018**, *52* (2), 115−120.

(3) Anandan, A.; Vrielink, A. Structure and function of lipid A-modifying enzymes. *Ann. N.Y. Acad. Sci.* **2020**, *1459*, 19−37.

(4) Bohan, Yu.; Qin, Li.; Zhou, M. LPS-induced upregulation of the TLR4 signaling pathway inhibits osteogenic differentiation of human periodontal ligament stem cells under inflammatory conditions. *Int. J. Mol. Med.* **2019**, *43*, 2341−2351.

(5) Shrivastava, R.; Chng, S.-S. Lipid trafficking across the Gram-negative cell envelope. *J. Biol. Chem.* **2019**, *294*, 14175−14184.

(6) Cucu, I. Signaling Pathways in Inflammation and Cardiovascular Diseases: An Update of Therapeutic Strategies. *Immuno.* **2022**, *2* (4), 630−650.

(7) El-Zayat, S. R.; Sibaii, H.; Mannaa, F. A. Toll-like receptors activation, signaling, and targeting: an overview. *Bull. Natl. Res. Cent.* **2019**, *43*, 187.

(8) Zhu, H.; Li, W.; Wang, Z.; Chen, J.; Ding, M.; Han, L. TREM-1 deficiency attenuates the inflammatory responses in LPS-induced murine endometritis. *Microb Biotechnol.* **2019**, *12* (6), 1337−1345.

(9) Fahmy, M. A.; Fattah, L. M. A.; Abdel-Halim, A. M.; Aly-Eldeen, M. A.; Abo-El-Khair, E. M.; Ahdy, H. H.; Ahdy, H. H.; Hemeilly, A.; El-Soud, A. A.; Shreadah, M. A. Evaluations of the Quality for the Egyptian Red Sea Coastal Waters during 2011−2013. *J. Environ. Prot.* **2016**, *7* (12), 1810−1834.

(10) Nabil-Adam, A.; Shreadah, M. A.; Abd El Moneam, N. M.; El-assar, S. A. *Pesudomance sp.* Bacteria Associated with Marine Sponge as a Promising and Sustainable Source of Bioactive Molecules. *Currr Pharm. Biotechnol.* **2019**, *20* (11), 964−984.

(11) Nabil-Adam, A.; Shreadah, M. A.; El Moneam, N. M. A.; El Assar, S. A. Various In Vitro Bioactivities of Secondary Metabolites Isolated from the Sponge *Hyrtios aff. Erectus* from the Red Sea Coast of Egypt. *Turk. J. Pharm. Sci.* **2020**, *17* (2), 127−135.

(12) Nabil-Adam, A.; Shreadah, M. A. Red Algae Natural Products for Prevention of Lipopolysaccharides (LPS)- induced liver and kidney inflammation and Injuries. *Biosci. Rep.* **2021**, *41*, BSR20202022.

(13) Nabil-Adam, A.; Shreadah, M. A. Anti-inflammatory, Antioxidant, Lung and Liver Protective Activity of *Galaxaura oblongata* as Antagonistic Efficacy against LPS using Hematological Parameters and Immunohistochemistry as Biomarkers. *Cardiovasc. Hematol. Agents Med. Chem.* **2022**, *20* (2), 148−165.

(14) Nabil-Adam, A.; Shreadah, M. A. Biogenic Silver Nanoparticles Synthesis from New Record Aquatic Bacteria of *Nile Tilapia* and Biological Activity. *J. Pure Appl. Microbiol.* **2020**, *14* (4), 2491−2511.

(15) Elissawy, A. M.; Soleiman Dehkordi, E.; Mehdinezhad, N.; Ashour, M. L.; Mohammadi Pour, P. Cytotoxic Alkaloids Derived from Marine Sponges: A Comprehensive Review. *Biomolecules* **2021**, *11*, 258.

(16) Nabil-Adam, A.; Ashour, M. L.; Tamer, T. M.; Shreadah, M. A.; Hassan, M. A. Interaction of *Jania rubens* polyphenolic extract as an antidiabetic agent with α-amylase, lipase, and trypsin: in vitro evaluations and in silico studies. *Catalysts* **2023**, *13* (2), 443.

(17) Shreadah, M. A.; El Moneam, N. M. A.; Al-Assar, S. A.; Nabil-Adam, A. Phytochemical and pharmacological screening of *Sargassium vulgare* from Suez Canal, Egypt. *Food Sci. Biotechnol.* **2018**, *27* (4), 963−979.

(18) Shreadah, M. A.; Aboul Ela, H. M.; Abdel Monem, N. M.; Yakout, G. A. Isolation, Phylogenetic Analysis of the Microbial Community Associated with the Red Sea Sponge *Ircinia Echinata* and Biological Evaluation of their Secondary Metabolites. *Biomed. J. Sci. Tech. Res.* **2018**, *12* (2), 9064−9082.

(19) Shreadah, M. A.; Abdel Moniem, N. M.; Yakout, G. A.; Aboul Ela, H. M. Bacteria from Marine Sponges: A Source of Biologically Active Compounds. *BioMedical: J. Sci. Tech. Res.* **2018**, *10* (5), 1−20.

(20) Shreadah, M. A.; Abd El Moneam, N. M.; El-Assar, S. A.; Nabil-Adam, A. Metabolomics and Pharmacological Screening of *Aspergillus versicolor* Isolated from *Hyrtios Erectus* Red Sea Sponge; Egypt. *Curr. Bioact. Compd.* **2020**, *16* (7), 1083−1102.

(21) Nabil-Adam, A.; Shreadah, M. A.; Abd El-Moneam, N. M.; El-Assar, S. A. Marine Algae of the *Genus Gracilaria* as a Multi Products Source for different Biotechnological and Medical Applications. *Recent Pat. Biotechnol.* **2020**, *14* (3), 203−228.
(22) Nabil-Adam, A.; Ashour, M. L.; Shreadah, M. A. The hepatoprotective candidates by synergistic formula of marine and terrestrial against Acetaminophen toxicity using in-vitro, in-vivo, and in silico screening approach. *Saudi J. Biol. Sci.* **2023**, *30* (4), 103607.
(23) Skrzypczak-Wiercioch, A.; Sałat, K. Lipopolysaccharide-Induced Model of Neuroinflammation: Mechanisms of Action, Research Application and Future Directions for Its Use. *Molecules.* **2022**, *27* (17), 5481.
(24) Chacón-Aponte, A. A.; Durán-Vargas, ÉA; Arévalo-Carrillo, J. A.; Lozada-Martínez, I. D.; Bolaño-Romero, M. P.; Moscote-Salazar, L. R.; Grille, P.; Janjua, T. Brain-lung interaction: a vicious cycle in traumatic brain injury. *Acute Crit. Care.* **2022**, *37* (1), 35−44.
(25) Di Meo, S.; Reed, T. T.; Venditti, P.; Victor, V. M. Role of ROS and RNS Sources in Physiological and Pathological Conditions. *Oxid. Med. Cell Longev.* **2016**, 1245049.
(26) Yuki, K.; Fujiogi, M.; Koutsogiannaki, S. COVID-19 pathophysiology: A review. *Clin immunol (Orlando, Fla.).* **2020**, *215*, 108427.
(27) Domscheit, H.; Hegeman, M. A.; Carvalho, N.; Spieth, P. M. Molecular Dynamics of Lipopolysaccharide-Induced Lung Injury in Rodents. *Front. Physiol.* **2020**, *11*, 36.
(28) Zhang, X.; Li, N.; Shao, H.; Meng, Y.; Wang, L.; Wu, Q.; Yao, Y.; Li, J.; Bian, J.; Zhang, Y.; Deng, X. Methane limit LPS-induced NF-κB/MAPKs signal in macrophages and suppress immune response in mice by enhancing PI3K/AKT/GSK-3β-mediated IL-10 expression. *Sci. Rep* **2016**, *6*, 29359.
(29) Fang, H.; Liu, A.; Chen, X.; Cheng, W.; Dirsch, O.; Dahmen, U. The severity of LPS-induced inflammatory injury is negatively associated with the functional liver mass after LPS injection in rat model. *J. inflammation (London, U. K.)* **2018**, *15*, 21.
(30) Collins, P. E.; Mitxitorena, I.; Carmody, R. J. The Ubiquitination of NF-κB Subunits in the Control of Transcription. *Cells* **2016**, *5* (2), 23.
(31) Robertson, R. C.; Guihéneuf, F.; Bahar, B.; Schmid, M.; Stengel, D. B.; Fitzgerald, G. F.; Ross, R. P.; Stanton, C. The Anti-Inflammatory Effect of Algae-Derived Lipid Extracts on Lipopolysaccharide (LPS)-Stimulated Human THP-1 Macrophages. *Mar. Drugs* **2015**, *13* (8), 5402−5424.
(32) Lee, J. C.; Hou, M. F.; Huang, H. W.; Chang, F. R.; Yeh, C. C.; Tang, J. Y.; Chang, H. W. Marine algal natural products with anti-oxidative, anti-inflammatory, and anticancer properties. *Cancer Cell Int.* **2013**, *13* (1), 55.
(33) Hwang, J. H.; Oh, Y. S.; Lim, S. B. Anti-inflammatory activities of some brown marine algae in LPS-stimulated RAW 264.7 cells. *Food Sci. Biotechnol* **2014**, *23*, 865−871.
(34) Muhammad, T.; Ikram, M.; Ullah, R.; Rehman, S. U.; Kim, M. O. Hesperetin, a Citrus Flavonoid, Attenuates LPS-Induced Neuroinflammation, Apoptosis and Memory Impairments by Modulating TLR4/NF-κB Signaling. *Nutrients* **2019**, *11* (3), 648.
(35) Zarghi, A.; Arfaei, S. Selective COX-2 Inhibitors: A Review of Their Structure-Activity Relationships. *Iran. J. Pharm. Res.* **2011**, *10* (4), 655−683.
(36) Lou, L.; Zhou, J.; Liu, Y.; Wei, Y.; Zhao, J.; Deng, J.; Dong, B.; Zhu, L.; Wu, A.; Yang, Y.; Chai, L. Chlorogenic acid induces apoptosis to inhibit the inflammatory proliferation of IL-6-induced fibroblast-like synoviocytes through modulating the activation of JAK/STAT and NF-κB signaling pathways. *Exp. Ther. Med.;* **2016**, *11* (5), 2054−2060.
(37) Nabil-Adam, A.; Elnosary, M. E.; Ashour, M. L.; El-Moneam, N. M. A.; Shreadah, M. A. Flavonoids Biosynthesis in Plants as a Defense Mechanism: Role and Function Concerning Pharmacodynamics and Pharmacokinetic Properties. *Flavonoid Metabolism—Recent Advances and Applications in Crop Breeding*; IntechOpen, 2023.
(38) Zhang, X.; Huang, H.; Yang, T.; Ye, Y.; Shan, J.; Yin, Z.; Luo, L. Chlorogenic acid protects mice against lipopolysaccharide-induced acute lung injury. *Injury.* **2010**, *41* (7), 746−752.
(39) Shan, J.; Fu, J.; Zhao, Z.; Kong, X.; Huang, H.; Luo, L.; Yin, Z. Chlorogenic acid inhibits lipopolysaccharide-induced cyclooxygenase-2 expression in RAW264.7 cells through suppressing NF-kappaB and JNK/AP-1 activation. *Int. Immunopharmacol* **2009**, *9*, 1042−1048.
(40) Li, Y.; Deng, S. L.; Lian, Z. X.; Yu, K. Roles of Toll-Like Receptors in Nitroxidative Stress in Mammals. *Cells* **2019**, *8* (6), 576.
(41) Jiang, K.; Zhang, T.; Yin, N.; Ma, X.; Zhao, G.; Wu, H.; Qiu, C.; Deng, G. Geraniol alleviates LPS-induced acute lung injury in mice via inhibiting inflammation and apoptosis. *Oncotarget.* **2017**, *8*, 71038−71053.
(42) Yan, Y.; Li, Q.; Shen, L.; Guo, K.; Zhou, X. Chlorogenic acid improves glucose tolerance, lipid metabolism, inflammation and microbiota composition in diabetic db/db mice. *Front Endocrinol.* **2022**, *13*, 1042044.
(43) Ye, H. Y.; Jin, J.; Jin, L. W.; Chen, Y.; Zhou, Z. H.; Li, Z. Y. Chlorogenic Acid Attenuates Lipopolysaccharide-Induced Acute Kidney Injury by Inhibiting TLR4/NF-κB Signal Pathway. *Inflammation* **2017**, *40* (2), 523−529.
(44) Lu, Y.-h.; Hong, Y.; Zhang, T.-y.; Chen, Y.-x.; Wei, Z.-j.; Gao, C.-y. Rosmarinic acid exerts anti-inflammatory effect and relieves oxidative stress via Nrf2 activation in carbon tetrachloride-induced liver damage. *Food Nutr. Res.* **2022**, *66*, 36590857.
(45) Scheckel, K. A.; Degner, S. C.; Romagnolo, D. F. Rosmarinic Acid Antagonizes Activator Protein-1-Dependent Activation of Cyclooxygenase-2 Expression in Human Cancer and Nonmalignant Cell Lines. *J. Nutr.* **2008**, *138* (11), 2098−2105.
(46) Luo, C.; Zou, L.; Sun, H.; Peng, J.; Gao, C.; Bao, L.; Ji, R.; Jin, Y.; Sun, S. A Review of the Anti-Inflammatory Effects of Rosmarinic Acid on Inflammatory Diseases. *Front. Pharmacol* **2020**, *11*, 153.
(47) Wang, W.-J.; Cheng, M.-H.; Lin, J.-H.; Weng, C.-S. Effect of a rosmarinic acid supplemented hemodialysis fluid on inflammation of human vascular endothelial cells. *Braz. J. Med. Biol. Res.* **2017**, *50* (12). DOI: 10.1590/1414-431X20176145.
(48) Wang, J.; Fang, X.; Ge, L.; Cao, F.; Zhao, L.; Wang, Z.; Xiao, W. Antitumor, antioxidant and anti-inflammatory activities of Kaempferol and its corresponding glycosides and the enzymatic preparation of Kaempferol. *PloS One* **2018**, *13* (5), No. e0197563.
(49) Ju, Z.; Li, M.; Xu, J.; Howell, D. C.; Li, Z.; Chen, F.-E. Recent development on COX-2 inhibitors as promising anti-inflammatory agents: The past 10 years. *Acta Pharm Sin B.* **2022**, *12*, 2790−2807.
(50) Zhou, D.; Yang, Q.; Tian, T.; Chang, Y.; Li, Y.; Duan, L.-R.; Li, H.; Wang, S.-W. Gastroprotective effect of gallic acid against ethanol-induced gastric ulcer in rats: Involvement of the Nrf2/HO-1 signaling and anti-apoptosis role. *Biomed Pharmacother.* **2020**, *126*, 110075.
(51) Landskron, G.; De la Fuente, M.; Thuwajit, P.; Thuwajit, C.; Hermoso, M. A. Chronic inflammation and cytokines in the tumor microenvironment. *J. immunol. Res.* **2014**, *2014*, 149185.
(52) Desai, S. J.; Prickril, B.; Rasooly, A. Mechanisms of Phytonutrient Modulation of Cyclooxygenase-2 (COX-2) and Inflammation Related to Cancer. *Nutr. Cancer* **2018**, *70* (3), 350−375.
(53) Zappavigna, S.; Cossu, A. M.; Grimaldi, A.; Bocchetti, M.; Ferraro, G. A.; Nicoletti, G. F.; Filosa, R.; Caraglia, M. Anti-Inflammatory Drugs as Anticancer Agents. *Int. J. Mol. Sci.* **2020**, *21*, 2605.
(54) Djuricic, I.; Calder, P. C. Beneficial Outcomes of Omega-6 and Omega-3 Polyunsaturated Fatty Acids on Human Health: An Update for 2021. *Nutrients* **2021**, *13*, 2421.
(55) Balić, A.; Vlašić, D.; Žužul, K.; Marinović, B.; Bukvić Mokos, Z. Omega-3 Versus Omega-6 Polyunsaturated Fatty Acids in the Prevention and Treatment of Inflammatory Skin Diseases. *Int. J. Mol. Sci.* **2020**, *21* (3), 741.
(56) Ahmad, T. B.; Rudd, D.; Kotiw, M.; Liu, L.; Benkendorff, K. Correlation between Fatty Acid Profile and Anti-Inflammatory Activity in Common Australian Seafood by-Products. *Mar. Drugs* **2019**, *17* (3), 155.

(57) Huerta-Yépez, S.; Tirado-Rodriguez, A. B.; Hankinson, O. Role of diets rich in omega-3 and omega-6 in the development of cancer. *Bol Med. Hosp Infant Mex.* **2016**, *73* (6), 446−456.
(58) Crowe, W.; Allsopp, P. J.; Nyland, J. F.; Magee, P. J.; Strain, J.J.; Doherty, L. C.; Watson, G. E.; Ball, E.; Riddell, C.; Armstrong, D. J.; Penta, K.; Todd, J. J.; Spence, T.; McSorley, E. M. Inflammatory response following in vitro exposure to methylmercury with and without n-3 long chain polyunsaturated fatty acids in peripheral blood mononuclear cells from systemic lupus erythematosus patients compared to healthy controls. *Toxicol. in Vitro* **2018**, *52*, 272−278.
(59) Wang, L.; Pan, X.; Jiang, L.; Chu, Y.; Gao, S.; Jiang, X.; Zhang, Y.; Chen, Y.; Luo, S.; Peng, C. The Biological Activity Mechanism of Chlorogenic Acid and Its Applications in Food Industry: A Review. *Front Nutr.* **2022**, *9*, 943911.
(60) Naveed, M.; Hejazi, V.; Abbas, M.; Kamboh, A. A.; Khan, G. J.; Shumzaid, M.; Ahmad, F.; Babazadeh, D.; FangFang, X.; Modarresi-Ghazani, F.; WenHua, L.; XiaoHui, Z. Chlorogenic acid (CGA): A pharmacological review and call for further research. *Biomed Pharmacother.* **2018**, *97*, 67−74.
(61) Cheng, N.; Liang, Y.; Du, X.; Ye, R. D. Serum amyloid A promotes LPS clearance and suppresses LPS-induced inflammation and tissue injury. *EMBO Rep.* **2018**, *19* (10), No. e45517.
(62) Gouwy, M.; De Buck, M.; Portner, N.; Opdenakker, G.; Proost, P.; Struyf, S.; Van Damme, J. Serum amyloid A chemoattracts immature dendritic cells and indirectly provokes monocyte chemotaxis by induction of cooperating CC and CXC chemokines<. *Eur. J. Immunol.* **2015**, *45* (1), 101−112.
(63) Murdoch, C. C.; Espenschied, S. T.; Matty, M. A.; Mueller, O.; Tobin, D. M.; Rawls, J. F. Intestinal Serum amyloid A suppresses systemic neutrophil activation and bactericidal activity in response to microbiota colonization. *PLoS Pathogens* **2019**, *15* (3), No. e1007381.
(64) Annema, W.; Nijstad, N.; Tölle, M.; de Boer, J. F.; Buijs, R. V.; Heeringa, P.; van der Giet, M.; Tietge, U. J. Myeloperoxidase and serum amyloid A contribute to impaired in vivo reverse cholesterol transport during the acute phase response but not group IIA secretory phospholipase A(2). *J. Lipid Res.* **2010**, *51* (4), 743−754.
(65) Levels, J. H.; Marquart, J. A.; Abraham, P. R.; van den Ende, A. E.; Molhuizen, H. O.; van Deventer, S. J.; Meijers, J. C. Lipopolysaccharide is transferred from high-density to low-density lipoproteins by lipopolysaccharide-binding protein and phospholipid transfer protein. *Infect. Immun.* **2005**, *73* (4), 2321−2326.
(66) Sureda, A.; Martorell, M.; Bibiloni, M.; Bouzas, C.; Gallardo-Alfaro, L.; Mateos, D.; Capó, X.; Tur, J. A.; Pons, A. Effect of Free Fatty Acids on Inflammatory Gene Expression and Hydrogen Peroxide Production by Ex Vivo Blood Mononuclear Cells. *Nutrients* **2020**, *12* (1), 146.
(67) Malle, E.; Sodin-Semrl, S.; Kovacevic, A. Serum amyloid A: an acute-phase protein involved in tumour pathogenesis. *Cell. Mol. Life Sci.* **2009**, *66* (1), 9−26.
(68) Luan, H.; Kan, Z.; Xu, Y.; et al. Rosmarinic acid protects against experimental diabetes with cerebral ischemia: relation to inflammation response. *J. Neuroinflammation* **2013**, *10*, 810.
(69) Duan, Y.; Gong, K.; Xu, S.; et al. Regulation of cholesterol homeostasis in health and diseases: from mechanisms to targeted therapeutics. *Sig Transduct Target Ther* **2022**, *7*, 265.
(70) Peckett, A.; Wright, D.; Riddell, M. The effects of glucocorticoids on adipose tissue lipid metabolism. *Metabolism: clinical and experimental.* **2011**, *60*, 1500−10.
(71) Alves-Bezerra, M.; Cohen, D. E. Triglyceride Metabolism in the Liver. *Compr Physiol.* **2017**, *8* (1), 1−8.
(72) Niu, Y. G.; Evans, R. D. Very-low-density lipoprotein: complex particles in cardiac energy metabolism. *J. Lipids.* **2011**, *2011*, 189876.
(73) van Bergenhenegouwen, J.; Kraneveld, A. D.; Rutten, L.; Garssen, J.; Vos, A. P.; Hartog, A. Lipoproteins attenuate TLR2 and TLR4 activation by bacteria and bacterial ligands with differences in affinity and kinetics. *BMC Immunol* **2016**, *17*, 42.
(74) de Deus, I. J.; Martins-Silva, A. F.; Fagundes, M. M. A.; Paula-Gomes, S.; Silva, F. G. D. E.; da Cruz, L. L.; de Abreu, A. R. R.; de Queiroz, K. B. Role of NLRP3 inflammasome and oxidative stress in hepatic insulin resistance and the ameliorative effect of phytochemical intervention. *Front. Pharmacol.* **2023**, *14*, 1188829 DOI: 10.3389/fphar.2023.1188829.
(75) Behl, T.; Upadhyay, T.; Singh, S.; Chigurupati, S.; Alsubayiel, A. M.; Mani, V.; Vargas-De-La-Cruz, C.; Uivarosan, D.; Bustea, C.; Sava, C.; Stoicescu, M.; Radu, A. F.; Bungau, S. G. Polyphenols Targeting MAPK Mediated Oxidative Stress and Inflammation in Rheumatoid Arthritis. *Molecules.* **2021**, *26* (21), 6570.
(76) Shreadah, M. A.; Said, T. O.; El Zokm, G.; Masoud, M. S. Physico-Chemical Characterititics of the Surficial Sediments along the Egyptian Red Sea Coasts. *Egyptian J. Aquat. Res.* **2008**, *34* (4), 16−34.
(77) Shreadah, M. A.; Masoud, M. S.; Said, T. O.; El Zokm, G. Application of IR, X-Ray, TGA and DTA to determine the mineral composition of the Sediments and study of reaction kinetics along the Egyptian Red Sea Coasts. *Egyptian J. Aquat. Res.* **2008**, *34* (2), 83−95.
(78) Shreadah, M. A.; Said, T. O.; Abd El Ghani, S. A.; Ahmed, A. M. Alkyllead and Alkyltin Species in different fishes collected from the Suez Gulf, Egypt. *Egyptian J. Aquat. Res.* **2008**, *34* (4), 64−73.
(79) Nabil-Adam, A.; Youssef, F. S.; Ashour, M. L.; Shreadah, M. A. Neuroprotective and nephroprotective effects of Ircinia sponge in polycyclic aromatic hydrocarbons (PAHs) induced toxicity in animal model: a pharmacological and computational approach. *Environ. Sci. Pollut. Res. Int.* **2023**, *30*, 82178.
(80) National institute of standard and technology (NIST). https://webbook.nist.gov/chemistry/ (accessed 30.09.2023).
(81) Uddin, R.; Saha, M. R.; Subhan, N.; Hossain, H.; Jahan, I. A.; Akter, R.; Alam, A. HPLC-Analysis of Polyphenolic Compounds in *Gardenia jasminoides* and Determination of Antioxidant Activity by Using Free Radical Scavenging Assays. *Adv. Pharm. Bull.* **2014**, *4* (3), 273−281.
(82) Amarowicz, R.; Naczk, M.; Zadernowski, R.; Shahidi, F. Antioxidant activity of condensed tannins of beach pea, Canola hulls, evening primrose, and faba bean. *J. Food Lipids.* **2000**, *7*, 195−205.
(83) Chakraborty, K.; Paulraj, R. Sesquiterpenoids with freeradical-scavenging properties from marine macroalga *Ulva fasciata* Delile,. *Food Chem.* **2010**, *122* (1), 31−41.
(84) Moyo, M.; Ndhlala, A. R.; Finnie, J. F.; Van Staden, J. Phenolic composition, antioxidant and acetylcholinesterase inhibitory activities of *Sclerocarya birrea* and *Harpephyllum caffrum* (*Anacardiaceae*) extracts. *Food Chem.* **2010**, *123*, 69−76.
(85) Fonteh, P. N.; Keter, F. K.; Meyer, D. New bis-(thiosemicarbazonate) gold (III) complexes inhibit HIV replication at cytostatic concentrations: potential for incorporation into virostatic cocktails. *J. Inorg. Biochem.* **2011**, *105*, 1173−1180.
(86) Enkhmaa, B.; Shiwaku, K.; Katsube, T.; Kitajima, T.; Anuurad, E.; Yamasaki, M.; Yamane, Y. (Mulberry *Morus alba L.*) leaves and their major flavonol quercetin 3-(6-malonylglucoside) attenuate atherosclerotic lesion development in LDL receptor-deficient mice. *J. Nutr.* **2005**, *135*, 729−734.
(87) Kumar, S.; Kaushik, N.; Proksch, P. Identification of antifungal principle in the solvent extract of an endophytic fungus *Chaetomium globosum* from *Withania somnifera*. *SpringerPlus* **2013**, *2*, 37.
(88) Lee, S. A.; Lee, S. H.; Kim, J. Y.; Lee, W. S. Effects of glycyrrhizin on lipopolysaccharide-induced acute lung injury in a mouse model. *J Thoracic Disease* **2019**, *11*, 1287−1302.
(89) Abd El-Moneam, N. M.; Al-Assar, S. A.; Shreadah, M. A.; Nabil-Adam, A. Isolation, Identification and Molecular Screening of Pseudomonas sp. Metabolic Pathways NRPs and PKS Associated with the Red Sea Sponge, *Hyrtios aff. Erectus*, Egypt. *J. Pure Appl. Microbiol.* **2017**, *11* (3), 1299−1311.
(90) Abd El-Moneam, N. M.; Shreadah, M. A.; El-Assar, S. A.; Nabil-Adam, A. Protective role of antioxidants capacity of *Hyrtios aff. Erectus* sponge extract against mixture of persistent organic pollutants (POPs)-induced hepatic toxicity in mice liver: biomarkers and ultrastructural study. *Environ. Sci. Pollut . Res.* **2017**, *24* (27), 22061−22072.
(91) Abd El Monein, N. M.; Yacout, G. A.; Aboul-Ela, H. M.; Shreadah, M. A. Hepatoprotective Activity of Chitosan Nanocarriers Loaded with the Ethyl Acetate Extract of *Astenotrophomonas sp.*

Bacteria Associated with the Red Sea Sponge *Amphimedon Ochracea* in CCl4 Induced Hepatotoxicity in Rats. *Adv. Biosci. Biotechnol.* **2017**, *8* (1), 27−50.
(92) Reitman, S.; Frankel, S. A colourimetric method for the determination of serum glutamate-oxaloacetate and pyruvate transaminases. *Am. J. Clin Pathol.* **1957**, *28*, 56.
(93) Doumas, B. T.; Ard Watson, W.; Biggs, H. G. Albumin standards and the measurement of serum albumin with bromcresol green. *Clin. Chim. Acta* **1971**, *31* (1), 87−96.
(94) Walters, M. I.; Gerarde, H. W. An ultramicromethod for the Determination of conjugated and total bilirubin in serum or plasma. *Microchem J.* **1970**, *15* (2), 231−243.
(95) Gornall, A. G.; Bardawill, C. J.; David, M. M. Determination of serum proteins by means of the biuret reaction. *J. Biol. Chem.* **1949**, *177* (2), 751−766.
(96) Henry, R. J.; Cannon, D. C.; Winkelman, J. W. *Clinical Chemistry: Principles and Technics*; Harper and Row: New York, 1974, p 541.
(97) Patton, C. J.; Crouch, S. R. Spectrophotometric and kinetics investigation of the Berthelot reaction for the Determination of ammonia. *Anal. Chem.* **1977**, *49*, 464−469.
(98) Zöllner, N.; Kirsch, K. Colorimetric Method for Determination of Total Lipids. *J. Experiment Med.* **1962**, *135*, 545−561.
(99) Bucolo, G.; David, H. Quantitative Determination of serum triglycerides by the use of enzymes. *Clin. Chem.* **1973**, *19* (5), 476−482.
(100) Allain, C. C.; Poon, L. S.; Chan, C. S.; Richmond, W.; Fu, P. C. Enzymatic Determination of total serum cholesterol. *Clin. Chem.* **1974**, *20* (4), 470−475.
(101) Koracevic, D.; Koracevic, G.; Djordjevic, V.; Andrejevic, S.; Cosic, V. Method for the measurement of antioxidant activity in human fluids. *J. Clin. Pathol.* **2001**, *54* (5), 356−361.
(102) Pulli, B.; Ali, M.; Forghani, R.; Schob, S.; Hsieh, K. L. C.; Wojtkiewicz, G.; Linnoila, J. J.; Chen, J. W. Measuring Myeloperoxidase Activity in Biological Samples. *PLoS One* **2013**, *8* (7), No. e67976.
(103) Griffith, J. Q.; Farris, E. J. *The Rat in Laboratory Investigation*; Lippincott: Philadelphia, 1942.
(104) Wang, B.; Song, N.; Yu, T.; Zhou, L.; Zhang, H.; Duan, L.; He, W.; Zhu, Y.; Bai, Y.; Zhu, M. Expression of Tumor Necrosis Factor-Alpha-Mediated Genes Predicts Recurrence-Free Survival in Lung Cancer. *PLoS One* **2014**, *9* (12), No. e115945.
(105) Yahaya, M. A. F.; Bakar, A. R. A.; Stanslas, J.; Nordin, N.; Zainol, M.; Mehat, M. Z. Insights from molecular docking and molecular dynamics on the potential of vitexin as an antagonist candidate against lipopolysaccharide (LPS) for microglial activation in neuroinflammation. *BMC Biotechnol.* **2021**, *21* (1), 38.
(106) Lipinski, C. A. Lead- and drug-like compounds: the rule-of-five revolution. *Drug Discov Today Technol.* **2004**, *1*, 337−341.
(107) Daina, A.; Michielin, O.; Zoete, V. SwissADME: a free web tool to evaluate pharmacokinetics, drug-likeness and medicinal chemistry friendliness of small molecules. *Sci. Rep.* **2017**, *7*, 42717.
(108) Muhammad, N.; Ahmad, M.; Sirajuddin, M.; Ali, Z.; Tumanov, N.; Wouters, J.; Chafik, A.; Solak, K.; Mavi, A.; Muhammad, S.; Shujah, S.; Ali, S.; Al-Sehemi, A. G. Synthesis, Characterization, Biological Activityand Molecular Docking Studies of Novel Organotin(IV) Carboxylates. *Front. Pharmacol.* **2022**, *13*, 864336.

https://doi.org/10.1021/acsomega.3c03480
ACS Omega 2023, 8, 37971−37990